Copolymerization Kinetics of Itaconic Acid and Acrylamide for the Application of Flocculants in Wastewater Treatment

By

Kiera Mathers

Submitted in partial fulfillment of the requirements
for the degree of Master of Applied Science

at

Dalhousie University
Halifax, Nova Scotia
November 2023

Table of Contents

List of Tables

List of Figures

Abstract

The objective of this thesis was to identify and evaluate a replacement for acrylic acid in the production of anionic polymer flocculants, which are used for treating inorganic contaminants such as silts and clays in wastewater. The replacement monomer that was investigated was itaconic acid (IA), which is produced from the fermentation of sugars instead of through petroleum-derived products. A design framework [1] was employed to determine whether itaconic acid could be utilized in the development of novel polymeric materials for the wastewater treatment industry.

The poly(itaconic acid-co-acrylamide) samples were successfully synthesized via aqueous solution polymerization using free radical polymerization. Design of experiments using the error-in-variables model [2] was employed to determine which comonomer ratios would provide the most information for reactivity ratio estimation. However, due to experimental challenges, additional comonomer ratios between 10 and 50 mol% itaconic acid were also tested. These polymer samples were then characterized using gravimetric analysis for conversion determination, elemental analysis for cumulative copolymer composition, gel permeation chromatography for molecular weight distribution and weight-average molecular weights, and zeta potential for net surface charge. Reactivity ratios were estimated using both the instantaneous and cumulative error-in-variables models, with the composition determined through elemental analysis. The cumulative reactivity ratios were found to be 1.4577 and 0.2914 for itaconic acid and acrylamide, respectively. These followed a similar trend to the literature [3, 4], which showed that itaconic acid has a reactivity ratio > 1 and acrylamide has a reactivity ratio < 1 for this copolymer system. In the current work, only two feed compositions (10 mol% and 20 mol% IA) yielded enough data to be used in reactivity ratio estimation; this limits the amount of information that can be gained about this copolymer system from the reactivity ratio estimates.

The highest feed fraction of itaconic acid to be successfully polymerized under the specific experimental parameters was 20 mol% itaconic acid (with the balance acrylamide), which translated to 35 mol% cumulative copolymer composition in the polymer product. A maximum weight-average molecular weight of 706 981 g/mol was achieved for this formulation at a conversion of 54.8 mass percent, which had a corresponding zeta potential of -31 mV. These itaconic acid / acrylamide copolymer samples were also compared to commercial anionic flocculant samples, which were tested to provide benchmark values for the novel polymer flocculants. The commercial samples all had weight-average molecular weights above 10 million g/mol and zeta potentials above -100 mV. These values are much larger than those of the novel itaconic acid and acrylamide copolymers, meaning there is still room for improvement of these new polymer flocculants. Recommendations for future work include investigating emulsion polymerization techniques to eliminate itaconic acid solubility challenges, and increasing the total monomer concentration. This could help drive the molecular weight averages closer to the commercial benchmarks as well as provide an easier scale-up, since emulsion polymerization is used more often in the industrial production of polymer flocculants. This research will help further the development of new climate-friendly flocculants that can be tailored to specific contaminants.

Acknowledgements

First, I would like to thank Dr. Alison Scott for her endless patience and support throughout this project. She has encouraged me to continually try new things, whether it was with research activities, outreach, or leadership opportunities, which has not only made me a better researcher but has also contributed to my personal growth.

I would like to convey my appreciation to the numerous individuals at Dalhousie University who have helped me through this degree. I had the pleasure of working with Dr. Saurabh Chitnis in Chemistry on the elemental analysis portion of my project, as well as with the Centre for Water Resource Studies for the application testing at Halifax water. I would also like to thank everyone in the Scott research group who have assisted with lab work and for providing encouragement, including Ian Conrod and Lindsay Sanderson.

Completing this thesis would not have been possible without the support of my friends and family. My parents, Dan and Marsha, have always inspired me to continue learning and to look at the world with curiosity. I'm extremely grateful for all of their love and support over the last two years! Lastly, I'm incredibly appreciative for my sister and all of my friends who have consistently cheered me on and provided space for me to relax when life gets a bit hectic.

Chapter 1. Introduction

1.1 Motivation

Water-soluble polymers play a crucial role in industrial wastewater treatment processes as coagulants and flocculants. Polymer flocculants are an important part of the treatment process since they can remove suspended solids and contaminants from the water in a significantly shorter time than if those solids were left to settle out naturally due to gravity [5]. The most commonly used polymers in these processes are charged polyacrylamides, which are made from acrylamide, a non-ionic monomer [6]. Acrylamide can be copolymerized with other (charged) monomers to form polyelectrolytes (cationic or anionic polymers), where the type of charge can be selected according to the properties of the solids being removed from the water [7]. One monomer that acrylamide (AAm) is commonly copolymerized with is acrylic acid (AAc), which forms an anionic copolymer [6]. Copolymers of acrylamide and acrylic acid can also be referred to as hydrolyzed polyacrylamide (HPAM). The anionic charges along the polymer backbone allow the flocculant to extend and uncoil due to charge repulsion along the polymer chain, and simultaneously provide a way for the flocculant to adsorb onto the contaminant particle surfaces by electrostatic attraction [8].

The aim of this research is to determine if acrylic acid can be replaced with a more sustainable alternative, such as itaconic acid, since the production of acrylic acid is dependent on petroleum processes. The polymerization procedures, product polymer properties, and flocculation ability will be evaluated for the design of novel anionic flocculants made with acrylamide and itaconic acid.

1.2 Objectives

One objective for this project was to design a polymerization procedure for the copolymer system of itaconic acid and acrylamide. This included determining the maximum monomer concentration, the initiator concentration, polymerization parameters such as temperature and pH, as well as developing an isolation procedure. Following the design of the polymerization procedure, the goal was to observe the reaction kinetics and characterize the resulting polymers, in order to optimize the production of climate-friendly anionic water-soluble polymer flocculants for wastewater treatment.

A secondary objective of this study was to demonstrate the applicability of the design framework proposed by Scott and Penlidis [1] in the design of polymer flocculants for wastewater treatment. This would be a novel use of the design framework and offers a promising strategy for enhancing the capability of these polymeric materials. Given the diverse nature of wastewater and the complexity of the contaminants that can be found within it, tailoring custom flocculants for specific contaminants could help to optimize the efficiency of flocculation processes.

1.3 Outline

This thesis is divided into 8 chapters, with a brief description of each chapter below.

Chapter 2 includes background information relevant to the work done in this project. It begins with an introduction to the design framework and how it is applied to the current study. Then, there is background information on the types of monomers used to produce anionic polymer flocculants,

as well as an overview of free radical polymerization with a focus on the copolymerization mechanism. A description of reactivity ratios and their importance copolymerization systems is then detailed. Next, the application requirements for polymer flocculants are explained, including the flocculation mechanism. Finally, the motivation for studying itaconic acid and the potential for customization of polymer products is described.

Chapter 3 details a case study that highlights two papers produced by Erbil et al. [3, 4]. Specifically, this chapter presents a comparison of the reactivity ratios that were calculated in the original papers, the re-estimated reactivity ratios (using the same techniques), and the error-in-variables model (EVM). This was done to demonstrate the variation in reactivity ratio estimation techniques and to show the justification for using EVM in the current project.

Chapter 4 describes the experimental methods used throughout the project. The materials used, polymer synthesis protocols, and polymer characterization methods are discussed.

Chapters 5 and 6 describe the experimental work performed and the results obtained. Chapter 5 focuses on the design of experiments and all of the preliminary experiments performed to better understand the itaconic acid / acrylamide copolymer system. It also demonstrates the results of reactivity ratio estimation using EVM and the new experimental data. Chapter 6 describes the optimization experiments, which include changing the initiator concentration in an effort to increase the molecular weight averages of the polymer product. Chapter 6 also details preliminary application testing for the synthesized polymers, with a comparison against commercially available flocculants using turbidity, zeta potential, and visual floc characterization.

Chapter 7 includes the conclusions drawn from the work done in this thesis, as well as recommendations for future work that is relevant to this thesis.

Appendix A contains sample calculations, including experimental design and composition calculations as well as relevant data sets for this project. Appendix B details the experiments using nuclear magnetic resonance (^{1}H-NMR) spectroscopy to validate itaconic acid incorporation into the synthesized copolymers.

Chapter 2. Background Information

2.1 Design Framework

This project aims to demonstrate the benefits of using a design framework for the design of new polymeric materials, as seen in Figure 2.1 [1]. This design framework uses a systematic and iterative approach to make informed design decisions, thereby reducing the amount of trial and error involved, and saving time and resources. The steps in the framework are intentionally fairly general, so that they can be applied to a wide variety of applications and industries. This framework has been used for case studies involving polymeric materials for enhanced oil recovery and for the detection of gas analytes [1], and could provide significant benefits through its novel application in the wastewater treatment industry due to the diverse and complex nature of contaminants that can be found in wastewater.

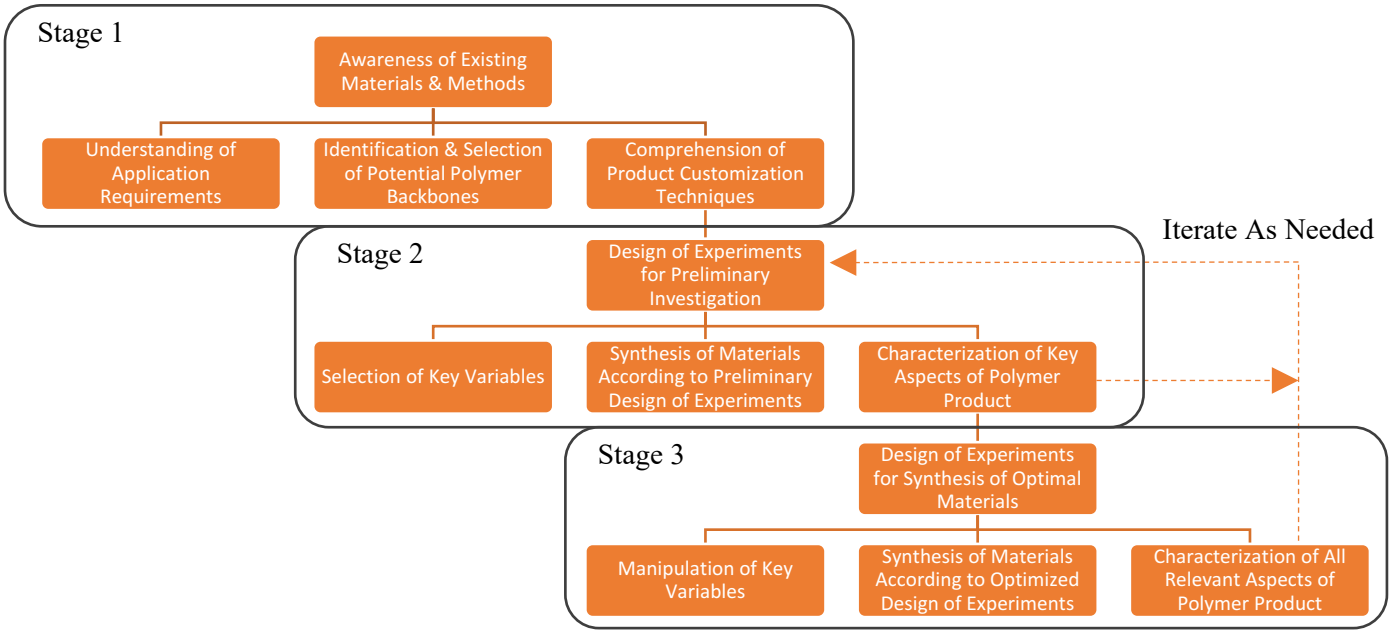

Figure 2.1: Design Framework Proposed by Scott and Penlidis (modified from [1])

The first stage consists of four steps which are intended to promote the development of prior knowledge, enhancing background understanding of what is available or currently being used for an application, before moving forward into designing experiments. Awareness of existing materials and methods relies on having prior knowledge due to experience or having access to databases describing which polymeric materials are being used for certain applications. This step can also help to identify where there is a gap in knowledge or room for improvement. Understanding the application requirements is crucial for the design process. Knowing where within an application the polymers are being used and what polymer properties will make them useful, such as their microstructure or molecular weight averages [1], will help inform which monomers and synthesis techniques could be used to produce polymers with those characteristics. Identifying potential polymer backbones requires an understanding of monomers available that can achieve those application requirements, such as producing high molecular weight polymers or copolymerizing different monomers to achieve a certain microstructure. Finally, identifying customization techniques requires an understanding of polymer reaction engineering and how changing the reaction parameters will impact the properties of the polymer.

The next four steps allow for the design and pursuit of the preliminary experiments required to understand the polymeric system using the background knowledge attained from the first steps. When designing new polymeric materials, there may not be a lot of previous experimental work available. While the first stage of the design framework relies on theory or predictions (or related work in other fields), the preliminary experiments aim to develop relationships between the key parameters identified through the customization step and the observed polymer properties. The design of experiments is performed to obtain the most information in the fewest experiments

possible. Key characteristics of the polymer are then chosen to be characterized and are selected based on which properties the customization techniques are expected to impact or which properties are expected to affect the polymers' application performance.

The final four steps allow for the synthesis procedure and polymer product to be optimized according to the specific application and product requirements. Either new formulations can be chosen based on the findings of the preliminary experiments, or one of the formulations can be chosen with new experimental parameters to tailor the final product (based on success criteria such as polymer properties or application performance). Preliminary experiments and product optimization can be iterated as needed, as more information about the system is obtained.

This design framework has been applied in the current study to show its potential for the design of polymeric materials in the application of wastewater treatment. The steps within the framework will be referenced throughout the thesis. Stage 1 is incorporated into the background section (Sections 2.2-2.5), Stage 2 is reflected in Chapter 5 for the preliminary experiments, and Stage 3 is seen in Chapter 6 for the optimization experiments.

2.2 Existing Materials and Methods

Commercial polymer flocculants can be made from a variety of monomers, which can impart different properties to the flocculant. The application of interest for this project was the application of anionic polymer flocculants for wastewater treatment. Anionic flocculants are often used to treat wastewater containing inorganic pollutants such as silts, clays, and various chemical contaminants [5, 9, 10], as well as municipal wastewaters [6]. Commercial anionic flocculants typically contain

(non-ionic) acrylamide and (anionic) acrylic acid. Acrylamide and acrylic acid, seen in Figure 2.2, are often used because they are inexpensive and very reactive, so they can produce long chain, high molecular weight polymers fairly quickly [8].

Figure 2.2: a) Acrylamide Structure [11] b) Acrylic Acid Structure [12]

Acrylamide/acrylic acid (AAm/AAc) based polymers have been widely used as flocculant and coagulant aids, and there has been a fair amount of research done on this polymer system. Recent studies have been looking at improving the biodegradability of AAm/AAc polymers by grafting them with bio-based polymers such as chitosan [9], starch [13], and gum ghatti [14]. Acrylamide in its monomer form has been identified as a possible carcinogen to humans [15], and there are some concerns about the polymer form degrading into its monomer form over time. However, the focus of this study was to replace the acrylic acid component, with future work dedicated to finding replacements for acrylamide. One major issue with acrylic acid is that the main feedstock for the monomer is partially oxidized propene, which is a by-product of petroleum processes [16]. As alternative energy sources are pursued, there also needs to be a plan to replace the materials that are derived from petroleum processes.

Most polymer flocculants are synthesized through free radical polymerization to create polymers with high molecular weight averages, on the order of 10^6 g/mol [6]. These high molecular weight averages make the polymers suitable for forming large aggregates, or flocs, at low dosages. Most of the commercially available polymer flocculants in wastewater treatment are synthesized via solution or emulsion free radical polymerization, as these techniques are cost effective and versatile [6]. Solution polymerization involves the dissolution of the desired monomers into a non-reactive solvent (in the case of the current study, it was water), along with the initiator. Emulsion polymerization involves the emulsification of hydrophobic monomers through an aqueous phase, with the generation of free radicals using a water-soluble initiator [17].

2.3 Application Requirements

Operators often have limited information about the properties of commercial polymer flocculants being used for wastewater treatment; this is due to the fact that the material specifications provided by manufacturers are typically not comprehensive. The information provided could include the polyelectrolyte type, such as if it is anionic or cationic, the percent ionization, and/or the average molecular weight of the polymer. However, not all of this information is known for each commercially available product. This means that to design new flocculants, an understanding of desirable polymer characteristics for the specific application is crucial. It also means that understanding the characteristics of polymer flocculants that are currently being used in industry is important for setting benchmark values to evaluate newly developed flocculants. Therefore, a study on commercial flocculants was completed for this thesis and is reported in Section 5.3.1.

There are several ways to treat wastewater, including membrane filtration, flotation, coagulation, and flocculation [18]. Polymers are used in the flocculation step, sometimes with the addition of a coagulant. Coagulants are typically inorganic metal salts such as aluminum sulphate [18], but they can also be short chain polyelectrolytes (that is, low molecular weight, charged polymers) [6]. Flocculation is generally understood as the aggregation of solids through the formation of bridges between particles to form flocs [6, 19]. Coagulation is sometimes required prior to the flocculation step to aid in destabilizing the particles in the wastewater and to form smaller aggregates that can then form flocs [19]. Coagulants are able to form small flocs on their own, however they are fragile and reversible, so polymer flocculants are typically used alongside coagulants to increase floc stability [20].

2.3.1 Flocculation Requirements

Short chain polyelectrolytes can be used as coagulants through two different charge neutralization mechanisms. They can either induce flocculation by compression of the double layer thickness, which increases the Van der Waals attraction forces and allows the particles to aggregate, as seen in Figure 2.3 and Figure 2.5, or they can create areas of opposite charges on the surface of the particles, allowing them to aggregate when in contact with other particle surfaces [6].

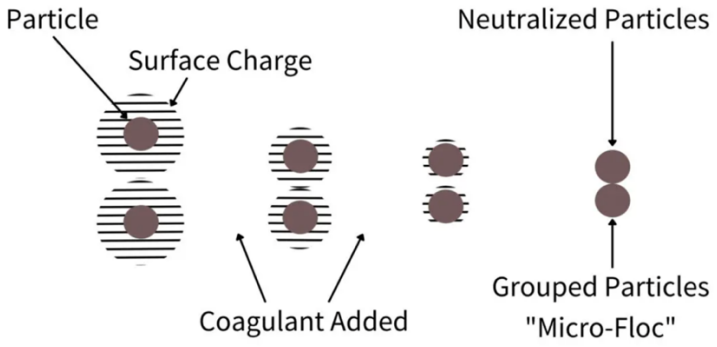

Figure 2.3: Visualization of a Coagulant Reducing the Surface Charge of a Particle [5]

Flocculation is achieved through the formation of bridges between particles through the electrical double layer. Bridging can occur when an adsorbed polymer chain is at least twice the length of the thickness of the electrical double layer, meaning it is long enough to extend its segments into the solution, where it can access more than one particle [6]. This is one of the reasons why polymer flocculants are typically high molecular weight, long chain polymers [8]. The goal is for the polymer to agglomerate small, suspended solids into larger ones, forming longer particle chains which become heavy and settle out of the water as they become visible to the naked eye [5]. This can be seen with the black line attaching three separate particles in Figure 2.4.

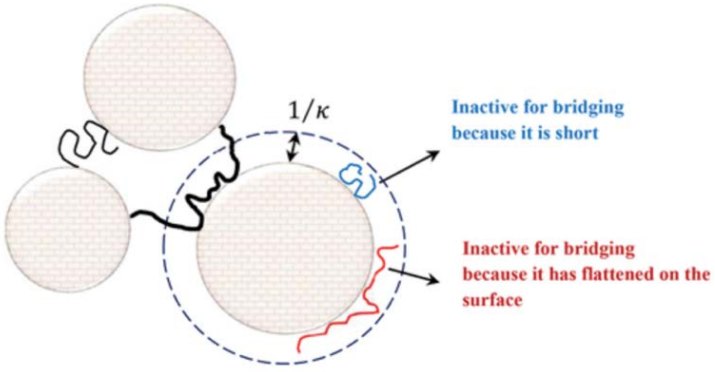

Figure 2.4: Flocculant Bridging Mechanism [6]

With high molecular weight polyelectrolytes, both charge neutralization and bridging can occur during flocculation [6]. Figure 2.5 shows both the coagulation (1a, 1b, and 1c) and flocculation (2a and 2b) steps to further demonstrate how large flocs can be formed.

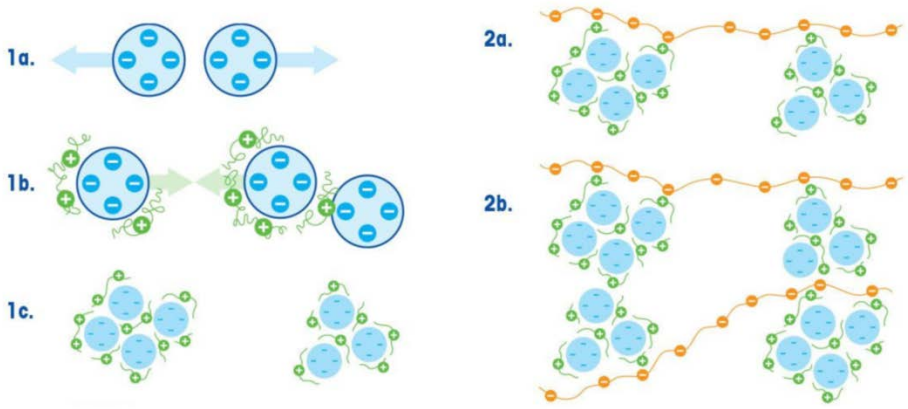

Figure 2.5:Coagulation through Opposite Charges (Step 1) and Flocculation (Step 2) Processes [19]

2.3.2 Fundamental Polymer Properties

As previously mentioned, high molecular weight averages are desired for flocculation applications, since long chains are better able to attach to numerous particles in the water; many flocculants have weight-average molecular weights over 10^6 g/mol [6]. An added benefit of high molecular weight polymers is that they can aid in decreasing flocculant dosage requirements. The charged components of the polymer flocculants, or the amount of charged monomer incorporated into the copolymers, promote adsorption onto the particle surfaces through electrostatic attraction, and the polymer molecules are able to uncoil and extend past the electrical double layer due to the charge repulsion along the polymer chain [8].

Another polymer property that is useful is the polydispersity index (PDI). The PDI is defined as the ratio between the weight-average molecular weight ($\overline{M_w}$) and the number-average molecular weight ($\overline{M_n}$), which can be seen in Equation 2.1 [17].

$$PDI = \frac{\overline{M_w}}{\overline{M_n}} \tag{2.1}$$

$$\overline{\mathrm{M_w}} = \sum w_i M_i \tag{2.2}$$

$$\overline{\mathrm{M_n}} = \sum x_i M_i \tag{2.3}$$

The $\overline{M_w}$ depends on the weight fraction, w_i, of chains with molecular weight M_i (Equation 2.2), whereas the $\overline{M_n}$ is determined by the mole fraction, x_i, of chains with molecular weight M_i (Equation 2.3) [17]. The PDI can help to determine how broad the distribution of chain lengths is within a polymer sample.

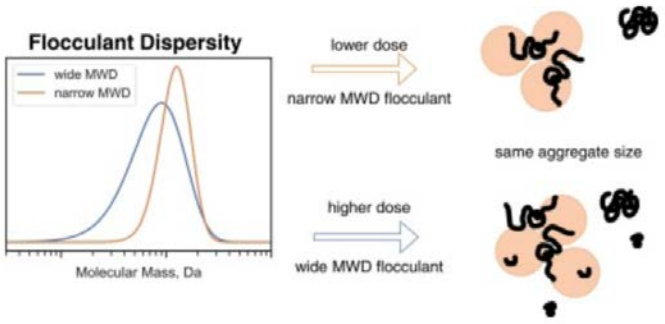

Figure 2.6: Comparison of Wide MWD (High PDI) versus Narrow MWD (Low PDI) and Impact on Flocculation Efficiency [21]

Figure 2.6 compares the flocculation efficiency of polymers with narrow and wide molecular weight distributions. A narrow MWD allows the dosage of the flocculant to be decreased, since the majority of the chains are able to participate in the bridging mechanism shown in Figure 2.4.

In contrast, flocculants with a wide MWD will include many short chains that are not able to participate in the flocculation mechanism. It should also be noted that when manufacturers report the molecular weights of their polymer products, they do not always specify which molecular weight characteristic (such as $\overline{M_w}$ or $\overline{M_n}$, or a peak molecular weight) is being reported, nor do they provide PDI estimates.

The microstructure of the polymer can also impact the ability of the flocculant to adsorb onto the particles. It has been seen that block copolymers, where there are long sections of one monomer and then the other, can be beneficial for flocculation. Compared to random or alternating microstructures, it provides more efficient use of the charged components of the copolymer, as seen in Figure 2.7 [6]. This will not be explored in this study; however it shows the importance of understanding how the comonomers are being incorporated into the copolymer.

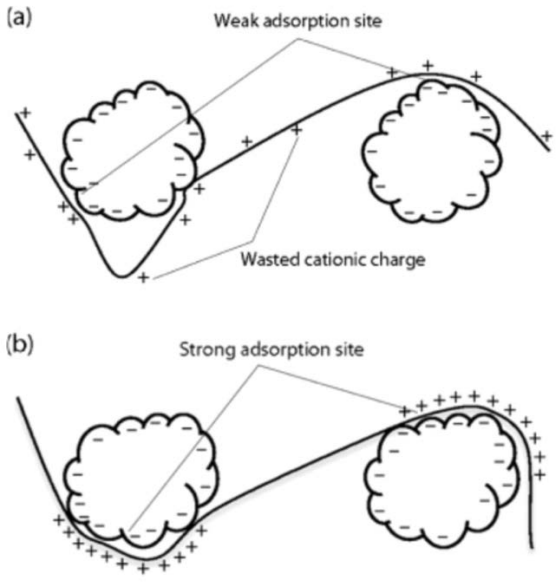

Figure 2.7: Comparison of (a) Random Copolymers versus (b) Block Copolymers for Flocculation [6]

2.4 Itaconic Acid and Acrylamide as a Potential Polymer Backbone

2.4.1 Itaconic Acid

Itaconic acid (IA) is a promising and sustainable alternative to acrylic acid. Itaconic acid is typically produced through the fermentation of sugars, which can also be sourced from biowaste [22] and can more readily biodegrade [23]. Itaconic acid has been identified as a possible alternative to acrylic acid due to similarities in chemical structure, as seen in Figure 2.8, including an unsaturated carboxyl group [22]. Itaconic acid has two carboxyl groups, with pkA values of 3.85 and 5.45 [24]. Itaconic acid also has a limited solubility in water: 8.31 g/100 mL at 20 °C [25]. This is a limitation for this study, as it limits the monomer concentration that is achievable in pre-polymerization formulations, and subsequently limits the molecular weight averages that can be achieved. For the preliminary studies, as seen in Chapter 5, the monomer concentration was kept constant for the different feed compositions tested. This meant that with the highest feed composition being $f_{IA,0}$=0.54, the highest monomer concentration that was achievable in the preparation of the monomer stock solution was only 1 M. This also limited the options available for optimizing the formulation, the details of which can be found in Chapter 6.

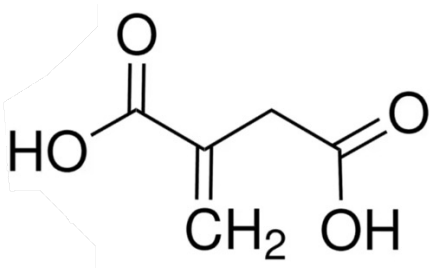

Figure 2.8: Itaconic Acid Structure [26]

The extra carboxyl group also makes it more difficult for the vinyl group to be opened by the radicals, since the carboxyl group makes the IA structure bulkier than acrylic acid. This likely slows down the rate of polymerization [27], meaning that it will take longer to achieve the same levels of conversion compared to acrylamide and acrylic acid copolymers.

There has been a recent interest in itaconic acid since it can be sourced from renewable resources and can be used to produce a variety of polymers for different applications such as a scale inhibitor for $CaCO_3$ [28], antibacterial food packaging [29], epoxy resins [30], and other industrial applications including water purification and flocculation [27]. Itaconic acid has specifically shown a lot of promise within the biomedical and pharmaceutical industries. This is due to IA being non-toxic, biocompatible, and biodegradable, as well as having antimicrobial properties [31]. There have also been a number of studies on the production of itaconic acid, which can already be produced on an industrial scale by the fermentation of carbohydrates using certain fungi [27] and can be optimized specifically with *Aspergillus terreus* [32, 33].

2.4.2 Itaconic Acid Copolymers

The majority of the research to date about itaconic acid is related to the polymer properties that can be obtained through different copolymerization's of itaconic acid; including with chitin, acrylonitrile, and acrylic acid [34, 35, 36]. Mostafa et al. found that grafting itaconic acid onto chitin improved the resulting copolymer's thermal stability in comparison to chitin homopolymers [34]. It was also seen that acrylonitrile and itaconic acid copolymers could be produced, with optimized molecular weights and viscosities achievable by using solution polymerization of acrylonitrile and itaconic acid in a mixture of dimethylsulfoxide (DMSO) and ultra-high molecular

weight poly(acrylonitrile) (UHMWPAN) as the solvent [35]. Acrylic acid and itaconic acid, in a ratio of 70:30 due to solubility limitations of itaconic acid, were successfully polymerized using photopolymerization with thioglycolic acid (TGA) as a chain transfer agent [36]. This system showed that itaconic acid incorporated at a higher amount in comparison to the feed composition and achieved weight-average molecular weights around $1.5 \cdot 10^5$ g/mol with PDIs between 2.45 and 1.62. This study showed the possibility of tailoring the molecular weights and viscosities of the acrylic acid and itaconic acid copolymers by adjusting the TGA content in the feed.

However, there appear to be only a limited number of studies working to understand the kinetics of itaconic acid copolymerization [24, 37, 38]. A paper published by Cummings et al. [24] observed the kinetics of acrylic acid and itaconic acid. They tested feed compositions of $f_{IA,0} = 0.1$, 0.13, and 0.25 due to solubility limitations of itaconic acid and reached a maximum conversion of 21.7%, 15.4% and 9.93% within 300 minutes for each respective feed composition. They also saw that itaconic acid incorporated at a higher proportion in comparison to the feed composition and determined reactivity ratios using the error-in-variables model to be 1.62 for itaconic acid and 0.36 for acrylamide. Erbil et al. [38] looked at a copolymer system of N-isopropylacrylamide (NIPAAm) and itaconic acid and determined the reactivity ratios using a variety of linear graphical methods including Fineman-Ross and Kelen-Tüdös. These methods found the reactivity ratios to be between 0.89 and 1.89 for NIPAAm and between 0.016 and 0.64 for itaconic acid. They also found that this system was not ideal for copolymerization and reported difficulties determining copolymer composition which would impact the reactivity ratio estimations.

The copolymerization of itaconic acid and acrylamide has been researched, however the focus of most studies has been on the application of superabsorbent hydrogels [39, 40, 41]. These studies were focused on crosslinking polymerization and modifying gel strength through the addition of other components to the copolymer. The copolymerization kinetics of itaconic acid and acrylamide have not been thoroughly studied, so one aim of this thesis was to provide accurate reactivity ratios for this polymer system. There were two kinetic studies conducted by Erbil et al. in 1999 and 2000 [3, 4], however these seem to be the only studies to date that focus on copolymerization kinetics for this system. These studies are investigated in depth in Chapter 3.

2.5 Product Customization Techniques

Since these polymers are being synthesized specifically for this project, there is significant potential to customize the product. Certain parameters such as the monomer concentration and the initiator concentration will impact the molecular weight averages of the polymers, the types of monomers being used will impact the polyelectrolyte type, and the reaction conditions such as temperature, pH, and time will determine the rate of polymerization and the conversion that can be attained from the polymer system.

2.5.1 Free Radical Polymerization

Free radical polymerization (FRP) is a type of chain-growth polymerization, which is composed of 3 main types of reactions: initiation, propagation, and termination. The reaction mechanisms are detailed in Table 2.1. Free radicals must be introduced to the system using an initiator. The rate of polymerization (R_p) is dependent on the rate of initiation (R_i), which is proportional to the

initiator concentration as seen in Equation 2.4. Here, f is the initiator efficiency, k_d is the initiator decomposition rate constant, and [I] is the initiator concentration [17].

$$R_i = 2fk_d[I] \tag{2.4}$$

Using the steady state assumption, where the rate of initiation is equal to the rate of termination, the rate of polymerization is proportional to the monomer concentration and the square root of the initiator concentration, as seen in Equation 2.5. Here, k_p is the propagation rate constant, k_t is the termination rate constant, and [M] is the monomer concentration.

$$R_p = k_p[M]\left(\frac{fk_d[I]}{k_t}\right)^{\frac{1}{2}} \tag{2.5}$$

Table 2.1: FRP Mechanism

Reaction Type	Mechanism
Initiation	$I \xrightarrow{k_d} 2R\cdot$ $R\cdot + M \xrightarrow{k_i} M\cdot$
Propagation	$M\cdot + M \xrightarrow{k_p} M-M\cdot$ $M-M\cdot + M \xrightarrow{k_p} M-M-M\cdot$ . . $M_n\cdot + M \xrightarrow{k_p} M_{n+1}\cdot$
Termination (by Combination)	$M_n\cdot + M_m\cdot \xrightarrow{k_{tc}} M_{n+m}$
Termination (by Disproportionation)	$M_n\cdot + M_m\cdot \xrightarrow{k_{td}} M_n + M_m$

Note that n and m are denoting radical chains of different lengths combining.

Free radical polymerization is a well-studied process, and it is understood that for the majority of free radical polymerizations, the mode of termination is by combination, which is where two radicals combine to form an electron pair [17].

The propagation step for copolymerization is a bit more complicated than what is shown in Table 2.1 due to the addition of a second comonomer. Instead of the growing radical chain only having the option to attach to one monomer, there are 4 possible combinations that could occur. This is according to the terminal model proposed by Mayo and Lewis, which states that the reactivity of the active site ($M\cdot$) is determined only by the nature of the terminal monomer [17]. The four possible reactions are depicted below, where k_{ij} represents the propagation rate constants for different combinations of comonomers.

$$\sim\sim M_1\cdot + M_1 \xrightarrow{k_{11}} \sim\sim M_{11}\cdot$$

$$\sim\sim M_1\cdot + M_2 \xrightarrow{k_{12}} \sim\sim M_{12}\cdot$$

$$\sim\sim M_2\cdot + M_2 \xrightarrow{k_{22}} \sim\sim M_{22}\cdot$$

$$\sim\sim M_2\cdot + M_1 \xrightarrow{k_{21}} \sim\sim M_{21}\cdot$$

2.5.2 Reactivity Ratio Estimation

Reactivity ratios describe the degree of incorporation of two comonomers into the resulting copolymer, and the reactivity ratios of two comonomers can sometimes differ substantially. When the comonomers have different reactivity ratios, the concentration of the more readily incorporated comonomer will drop more quickly than the concentration of the other comonomer, which causes

a composition drift inside the reactor [6]. Therefore, calculating the reactivity ratios for a specific polymeric system provides critical information about the resulting copolymers.

Reactivity ratios, r_i, represent the likelihood of homopropagation relative to crosspropagation during the copolymer synthesis, as seen in Equations 2.6 and 2.7 [42]. The right-hand side of the equations show the ratio of the propagation rate constants, k_{ij} (monomer *j* adding to macroradical *i*), which can be seen in the propagation reactions in Section 2.5.1.

$$r_1 = \frac{k_{11}}{k_{12}} \tag{2.6}$$

$$r_2 = \frac{k_{22}}{k_{21}} \tag{2.7}$$

Accurate reactivity ratio estimates are important for understanding copolymerization kinetics and producing copolymers for target applications. A variety of methods have been developed for reactivity ratio estimation and rely upon experimental data (namely, feed composition and composition of the copolymer product) obtained using multiple different feed compositions. Traditionally, linear models have been used for estimation since they contain simpler calculations; initially the technology was not available to solve the calculations required in non-linear methods. Linear models include the Mayo-Lewis method (or the method of intersections), the Fineman-Ross method, and the Kelen-Tüdös method [43]. These methods rely upon the instantaneous copolymer composition (ICC) model (Equation 2.8), which requires that the reaction must be kept at low conversions to maintain the assumption that composition drift is not occurring. This allows for the assumption that f_i is equal to $f_{i,0}$. The issue with this assumption is that at lower conversion there will be inherent variability, which will be demonstrated in Chapter 5. There is also the issue that there is no defined limit for what "low conversion" means, and it is up to the researcher to define

it for themselves. This could mean that some studies consider "low conversion" to be less than 10% and other studies to consider it to be less than 15%.

$$F_1 = \frac{r_1 f_1^2 + f_1 f_2}{r_1 f_1^2 + 2 f_1 f_2 + r_2 f_2^2} \tag{2.8}$$

The Mayo-Lewis method (or the method of intersections) employs Equation 2.9, which is a re-arranged version of the instantaneous copolymer composition equation.

$$r_2 = \frac{f_{1,0}}{f_{2,0}}\left(\frac{F_2}{F_1} - 1\right) + \frac{F_2 f_{1,0}^2}{F_1 f_{2,0}^2} r_1 \tag{2.9}$$

The mole fractions of each monomer (i) in the reaction feed (f_i, assumed to be equivalent to the comonomer feed composition ($f_{i,0}$)) and the mole fraction of each monomer incorporated into the copolymer (instantaneous copolymer composition, F_i) are needed to estimate reactivity ratios. The initial comonomer feed composition is known, with multiple different feed compositions chosen, and the instantaneous copolymer composition can be determined through experimental methods such as elemental analysis or nuclear magnetic resonance (NMR) spectroscopy. For the method of intersections, a theoretical r_2 is calculated for a range of r_1 values that can be determined from literature values. This is done for each of the experimental feed compositions used. The relationship between r_1 and r_2 is then plotted for each feed composition, and the experimental reactivity ratios for the copolymer system will theoretically lie where the lines intersect. A major issue with this method is that experimental error can prevent the lines from intersecting at one location, resulting in multiple points of intersection and inconsistent reactivity ratio estimates. This

makes it nearly impossible to determine which point of intersection is the most accurate for the system [43].

The Fineman-Ross approach also relies on a linear relationship, which is again based on the Mayo-Lewis equation. Fineman and Ross rearranged Equation 2.9 to form Equation 2.10, which produces one straight line from all feed and copolymer compositions. The left side of the equation is plotted against the right, where the resulting slope of the line is r_1 and $-r_2$ is the y-intercept [43].

$$\frac{f_{1,0}}{f_{2,0}}\left(1-\frac{F_2}{F_1}\right)=r_1\left(\frac{F_2}{F_1}\right)\left(\frac{f_{1,0}^2}{f_{2,0}^2}\right)-r_2 \tag{2.10}$$

A significant issue with this method is that it relies on one of the monomers being chosen as monomer 1, and that decision can impact the resulting reactivity ratio estimates. This is typically referred to as a lack of symmetry, where different reactivity ratios are determined based on the subjective nature of the researcher choosing how to define monomer 1 and monomer 2 [43].

The Kelen-Tüdös method is similar to the Fineman-Ross method, but also includes a correction factor (α), as seen in Equation 2.11, to help account for the fact that a linear relationship is used for a non-linear system. The correction factor improves the accuracy of the model and equally spaces the experimental data points along the x-axis. This helps to correct one of the limitations of the Fineman-Ross approach, where different reactivity ratios are calculated depending on which monomer is chosen as monomer 1 [43].

$$\alpha = \sqrt{\left(\frac{f_{1,0}^2}{f_{2,0}^2} * \frac{F_2}{F_1}\right)_{min} \left(\frac{f_{1,0}^2}{f_{2,0}^2} * \frac{F_2}{F_1}\right)_{max}} \tag{2.11}$$

This results in the following equation, which is used in the same way as the Fineman-Ross equation, with the left side being plotted against the right side. The resulting slope of the line is equal to $r_1 + \frac{r_2}{\alpha}$ and the intercept is equal to $-\frac{r_2}{\alpha}$ [43].

$$\frac{\left(\frac{f_{1,0}}{f_{2,0}}\right)\left(1-\frac{F_2}{F_1}\right)}{\alpha+\left(\frac{f_{1,0}^2}{f_{2,0}^2}\right)\left(\frac{F_2}{F_1}\right)} = \left(r_1 + \left(\frac{r_2}{\alpha}\right)\right)\frac{\left(\frac{f_{1,0}^2}{f_{2,0}^2}\right)\left(\frac{F_2}{F_1}\right)}{\alpha+\left(\frac{f_{1,0}^2}{f_{2,0}^2}\right)\left(\frac{F_2}{F_1}\right)} - \left(\frac{r_2}{\alpha}\right) \tag{2.12}$$

All three of the above methods are linear methods, and the major drawback to these is that both the independent and dependent variables contain the observed response, which is the copolymer composition. This introduces experimental error into all of the variables within the equations, on top of the inherent inaccuracy of the models attempting to linearize non-linear relationships. These models are most useful for providing an initial estimate of the reactivity ratios, which can then be used in a non-linear model such as Tidwell-Mortimer or the error-in-variables model, which will be described later in this section.

The extended Kelen-Tüdös method is a differential form of the Kelen-Tüdös method, which allows for the inclusion of experiments that go up to 40% conversion, by including new parameters which are related to the partial molar conversions of the monomers (f_1 and f_2) [43]. The updated equations are shown in Equations 2.13 and 2.14, with the same relationship being plotted as the Kelen-Tüdös method, shown by Equation 2.15 which is in the same form as Equation 2.12.

$$\varepsilon^C = \frac{\left(\frac{F_1}{F_2}\right)\left(\frac{\log\left(\frac{f_2}{f_{2,0}}\right)}{\log\left(\frac{f_1}{f_{1,0}}\right)}\right)^2}{\alpha+\left(\frac{F_1}{F_2}\right)\left(\frac{\log\left(\frac{f_2}{f_{2,0}}\right)}{\log\left(\frac{f_1}{f_{1,0}}\right)}\right)^2} \tag{2.13}$$

$$\eta^C = \frac{\left(\frac{F_1-F_2}{F_2}\right)\left(\frac{\log\left(\frac{f_2}{f_{2,0}}\right)}{\log\left(\frac{f_1}{f_{1,0}}\right)}\right)}{\alpha+\left(\frac{F_1}{F_2}\right)\left(\frac{\log\left(\frac{f_2}{f_{2,0}}\right)}{\log\left(\frac{f_1}{f_{1,0}}\right)}\right)^2} \tag{2.14}$$

$$\eta^C = \left(r_1 + \left(\frac{r_2}{\alpha}\right)\right)\varepsilon^C - \left(\frac{r_2}{\alpha}\right) \tag{2.15}$$

The curve fitting method provides an attempt at dealing with the nonlinear relationship defined by the terminal model and relies on the differential form of the instantaneous copolymer equation (recall Equation 2.8). This has been presented in Equation 2.16, where again f_1 and f_2 represent the mole fractions of comonomers in the reacting mixture [43].

$$\frac{df_1}{df_2} = \frac{F_1}{F_2} = \left(\frac{f_1}{f_2}\right)\left(\frac{r_1 f_1 + f_2}{f_1 + r_2 f_2}\right) \tag{2.16}$$

This method relies on choosing the curve that best represents $F_i = F(f_{i,0})$ for a given set of experimental data by varying the reactivity ratios, which are found using one of the previously mentioned linear methods. However, there is no objective criterion for choosing the "best fit" and the results are therefore up to the subjective decisions of individual researchers. Initial estimates for the reactivity ratios are calculated using either Fineman-Ross or Kelen-Tüdös, which are used in Equation 2.17 which is a rearranged version of the instantaneous copolymer composition model (Equation 2.8); the model results are then graphically compared to the experimental data [43].

$$F_1 = \frac{f_1^2(r_1-1)+f_1}{f_1^2(r_1+r_2-2)+2f_1(1-r_1)+r_2} \quad (2.17)$$

If the initial curve does not fit the experimental data, then a different pair of reactivity ratios is chosen, and the method is repeated until a suitable curve (using suitable reactivity ratio estimates) is found that adequately matches the experimental data [43].

The Tidwell-Mortimer approach uses non-linear least squares to estimate reactivity ratios and is an improved version of the curve fitting method. Initial estimates for r_1 and r_2 are determined again using the Fineman-Ross or Kelen-Tüdös methods, and then the model is refined through successive iterations to minimize the sum of mean square deviations. Typically, three iterations are sufficient if good initial estimates are used. However, the major shortcomings of this method are that initial estimates are required (which can be somewhat subjective), and that the method does not account for experimental error in the independent variable, the feed composition [43].

The error-in-variables model (EVM) is another non-linear method for estimating monomer reactivity ratios. A brief description will be presented here; for more detailed descriptions refer to Kazemi et al. [44]. The error-in-variables model is the most statistically accurate method for estimating reactivity ratios, as it takes into consideration the error for both the independent and dependent variables [42]. EVM is an extension of the Tidwell-Mortimer method, where the sum of the weighted squares of the residuals is to be minimized [43]. The EVM algorithm uses a nested-iterative approach, which is more computationally difficult, but with technological advances it is more accessible and easier to use [44]. Typically, estimates from the Kelen-Tüdös method are used

for the initial reactivity ratios [43]. In EVM, the nested-iterative loop includes an inner loop, Equation 2.18, that searches for the "true" values (ξ_i) of the independent variables (x_i), while taking the experimental error (ε_i) into account. Note that k is a constant that represents the magnitude of the error.

$$x_i = \xi_i(1 + k\varepsilon_i) \tag{2.18}$$

Meanwhile, the outer loop, Equation 2.19, is using a copolymerization model such as the ICC equation, Equation 2.8, or a cumulative copolymerization model [45] which relates the true variables to the predicted values.

$$g(\xi_i, \theta) = 0 \tag{2.19}$$

This nested-iterative approach aims to minimize the sum of squares between the observed and predicted values. This can be seen graphically in Figure 2.9, with the inner loop minimizing the horizontal distance between the experimental data points and the model and the outer loop minimizing the vertical distance between the experimental data points and the model.

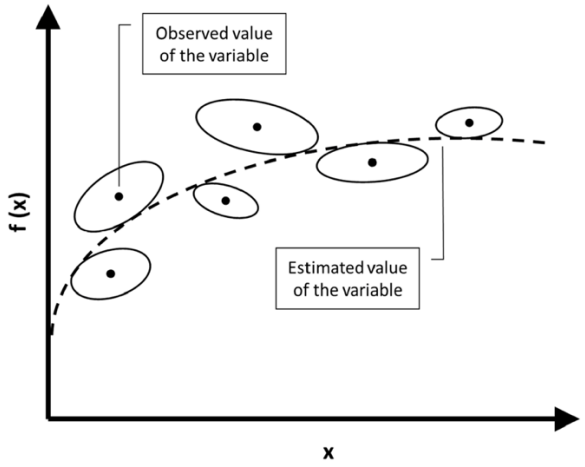

Figure 2.9: Graphical Representation of EVM [42]

2.5.3 Molecular Weight Relationships

From the relationship shown in Equation 2.20, the predicted $\overline{M_n}$ of a polymer sample can be manipulated through the monomer concentration and the initiator concentration.

$$\nu = \frac{k_p[M]}{2(fk_dk_t)^{\frac{1}{2}}[I]^{\frac{1}{2}}} \tag{2.20}$$

Here, ν is the kinetic chain length, which is equal to half of the number-average degree of polymerization ($\overline{DP_n}$) when termination is by combination. This is assumed for the current work, since termination by combination is common for most free radical polymerizations [17]. For vinyl polymers, the $\overline{DP_n}$ is equal the ratio of the $\overline{M_n}$ to the molecular weight of the monomer repeating unit (M_0), Equation 2.21. These relationships (recall Equation 2.5) mean that the number-average degree of polymerization is inversely proportional to the rate of polymerization at a given monomer concentration and temperature [17].

$$\overline{DP_n} = \frac{\overline{M_n}}{M_0} \tag{2.21}$$

Chapter 3. Reactivity Ratio Case Study

There is still much to learn about the itaconic acid/acrylamide copolymer system. There were two studies published by Erbil et al. in the early 2000s [3, 4] which compared multiple methods for estimating reactivity ratios, as well as two separate methods (conductometric and potentiometric titration) for determining the copolymer composition. Both methods used 0.1 g of the synthesized polymer dissolved in 30 mL of 0.1 N NaCl solution, and then titrated with 0.1 N NaOH. For the conductometric titration [3], the conductivity of the solutions was plotted versus the millilitres of titrant, and for the potentiometric titration [4], the pH of the solutions was plotted versus the millilitres of titrant. In both methods, the composition was determined from the inflection point of the curves.

The techniques for reactivity ratio estimation that were used in these papers were the Mayo-Lewis, Fineman-Ross, Kelen-Tüdös, extended Kelen-Tüdös, and Tidwell-Mortimer (which is also known as the non-linear least squares method (NLLS)) approaches. The authors used the same polymer synthesis methodology for both experiments, as well as the same experimental conditions. An overview of the initial feed compositions, conversions obtained during synthesis, and the copolymer compositions determined with both methods can be found in Table 3.1.

Table 3.1: Experimental Results for Itaconic Acid (IA)/Acrylamide (AAm) Copolymerization by Erbil et al. *[3, 4]*

Run No.	Initial monomer composition of IA ($f_{IA,0}$)	Conversion (%)	Copolymer Composition of IA (F_{IA})	
			Conductometric Titration [3]	Potentiometric Titration [4]
1	0.0984	13.80	0.16	0.16
2	0.2140	5.45	0.228	0.23
3	0.3531	8.89	0.403	0.40
4	0.5221	4.52	0.636	0.65
5	0.7320	2.42	0.796	0.75

Both studies used free radical polymerization in aqueous solution to synthesize the polymers. They used 1mM of potassium persulfate to initiate the reaction at 50°C under a nitrogen atmosphere. The reactions were allowed to proceed to low conversions, which the researchers defined as below 15%, by polymerizing between 20 to 60 minutes. However, the actual time for each specific run is not reported. The authors did not provide any information about how many replicates were completed, if any were done, or the number of samples that were included in each run. As presented, it seems that only one sample was synthesized for each run per study. It is also unclear whether the same synthesized samples were used for both studies, or if new materials were synthesized for each individual study. It is also interesting to note that the feed composition goes up to 73 mol% IA, since most studies that investigate itaconic acid polymerization do not use more than 30 mol% IA [24, 35, 36, 39, 40] due to solubility limitations of the monomer in water.

As shown in Table 3.1, the conversions reported for runs 2, 4, and 5 are quite low; run 5 is even below 3% conversion [3, 4]. This is such a low conversion that it could be considered noise, and without any replication information it is difficult to evaluate the accuracy of these data. It is also important to note that low conversion data typically include inherent variability. It is also important

to note that the exact same feed compositions and conversions were reported for both studies, which suggests that the same synthetic runs were applied to both analyses.

Both titration methods used by Erbil et al. [3, 4] measured the copolymer compositions to be very similar. Only the last two runs, numbers 4 and 5, showed slightly different results. The compositions themselves seem to be reasonable, with the itaconic acid being incorporated at a higher proportion than what is in the feed composition. This suggests that itaconic acid incorporates more readily at lower conversions until it is consumed, and then acrylamide will incorporate more readily in the copolymers. However, again, without any knowledge of replicates or number of samples, it is difficult to evaluate the accuracy of the results. However, the data presented by Erbil et al. [3, 4] rely on the assumption that these data are at low enough conversion to assume there is no composition drift, and that linear models can be used to estimate reactivity ratios. However, this assumption is flawed since there are significant differences between the feed composition and copolymer composition for at least 3 of the samples (run numbers 1, 3, and 4).

The data reported in Table 3.1 have been reanalyzed in the current work using the same reactivity ratio models reported in the original studies, including the Mayo-Lewis method of intersections, Fineman-Ross, Kelen-Tüdös, and extended Kelen-Tüdös techniques. These results were then compared to the values originally calculated and reported by Erbil et al. [3, 4]. The Tidwell-Mortimer method was not re-evaluated and was instead replaced by the error-in-variables model (to be described shortly). However, the Tidwell-Mortimer results reported by Erbil et al. are included here to promote comparison between the different estimation models. The re-calculated reactivity ratios were fairly close to what was reported originally, as can be seen in Table 3.2. All

reactivity ratio estimates (RREs) were then compared to reactivity ratios estimated using the error-in-variables model.

Table 3.2: Comparison of RREs Calculated in the Current Work and those Reported by Erbil et al. [3, 4]

	Conductometric Titration [3]				**Potentiometric Titration** [4]			
	Calculated		From the Literature		Calculated		From the Literature	
Method	r_{IA}	r_{AAm}	r_{IA}	r_{AAm}	r_{IA}	r_{AAm}	r_{IA}	r_{AAm}
Mayo-Lewis	1.25-1.35	0.40-0.55	1.38 ± 0.13	0.48 ± 0.08	0.90-1.10	0.50-0.95	1.38 ± 0.22	0.81 ± 0.10
Fineman-Ross	1.4691	0.7598	1.47 ± 0.03	0.76 ± 0.02	0.9907	0.5804	0.99 ± 0.04	0.58 ± 0.02
Kelen-Tüdös	1.2787	0.6735	1.25 ± 0.10	0.67 ± 0.05	1.0544	0.6231	1.05 ± 0.10	0.62 ± 0.06
Ext. Kelen-Tüdös	1.361	0.5654	1.24 ± 0.11	0.64 ± 0.05	1.0203	0.5915	1.02 ± 0.11	0.59 ± 0.06
Tidwell-Mortimer	-	-	1.65 ± 0.21	0.88 ± 0.08	-	-	1.36 ± 0.11	0.77 ± 0.06
EVM - Instantaneous	1.0731	0.6409	-	-	1.0054	0.6273	-	-
EVM - Cumulative	1.0623	0.6234	-	-	0.9914	0.6091	-	-

The overall trends for the reactivity ratios appear to agree between the different estimation models, with itaconic acid having a reactivity ratio around or greater than 1 (meaning it favours homo-propagation), and acrylamide having a reactivity ratio less than 1 (meaning it favours cross-propagation). The EVM results reported in Table 3.2 are the results from the instantaneous and cumulative models using just the data from each respective study. Figures 3.7 and 3.8 later in this section were created using the data from both studies together and the reactivity ratios will be discussed. Each of the methods used to re-analyze the data have been detailed below.

The first method that was re-analyzed was the Mayo-Lewis method, as shown in Figure 3.1. A collection of five lines was created to represent each experimental run (i.e., the five different feed compositions). This method resulted in poor intersection, with not all lines intersecting at a single value. This is a common challenge with this estimation technique, and means there is likely experimental error within the results. The lack of a single intersection could also be due to the fact that this model is trying to linearize a nonlinear relationship, resulting in a poor fit between the model and the experimental data.

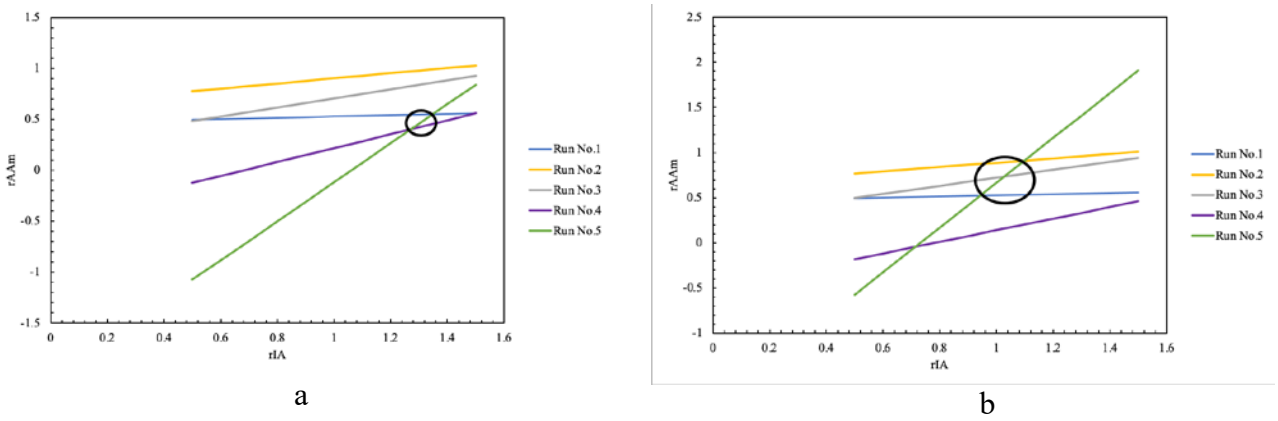

Figure 3.1: Mayo-Lewis Method of Intersection Results for the (a) Conductometric and (b) Potentiometric Studies

Due to the lack of a single intersection, a range of possible reactivity ratios was generated using this estimation model. Although this is not physically possible, since there should only be one "true" value for the reactivity ratios, this was done to attempt to compare the re-analyzed data to that reported by Erbil et al. [3, 4]. As shown in Table 3.2, the ranges of reactivity ratios were r_{IA}=1.25-1.35 and r_{AAm}=0.40-0.55 using the conductometric data, and r_{IA}=0.9-1.10 and r_{AAm}=0.50-0.95 using the potentiometric data. These were selected by identifying the area where the majority of the lines intersected, which included 3 lines for the conductometric study and 4 lines for the potentiometric study. The conductometric results align with what was reported by Erbil et al. [3], with the reported values lying within the range identified above. However, the potentiometric study determined that the r_{IA} value was smaller than that reported by Erbil et al. [4], with the reported value lying just outside of the range identified above. However, since the original authors do not discuss exactly how they calculated or selected the reactivity ratio estimates, this emphasizes the fact that this method is easily affected by the researcher's subjectivity and does not provide accurate reactivity ratio estimates.

Next the Fineman-Ross method was employed. Given the known concerns with estimation symmetry, both IA and AAm were defined as monomer 1 during separate estimations to determine how monomer definition impacts the estimation results. The results are shown in Figure 3.2. As expected, the choice of monomer 1 impacts the reactivity ratio estimations, particularly the reactivity ratio of itaconic acid.

An important note about all four relationships in Figure 3.2 is that the final data point, which is calculated from the first run (f_{IA}=0.0984), is skewing the trendline and seems to be more heavily

weighted in this estimation model. This is a known issue with this method since experimental data are unequally weighted in Equation 2.8 [43]. It should also be noted that the run 1 data point is the only sample that exceeded 10% conversion. Additionally, it is very clear that the lower conversion data do not follow a linear trend, which introduces doubt into these estimation results representing the "true" reactivity ratios.

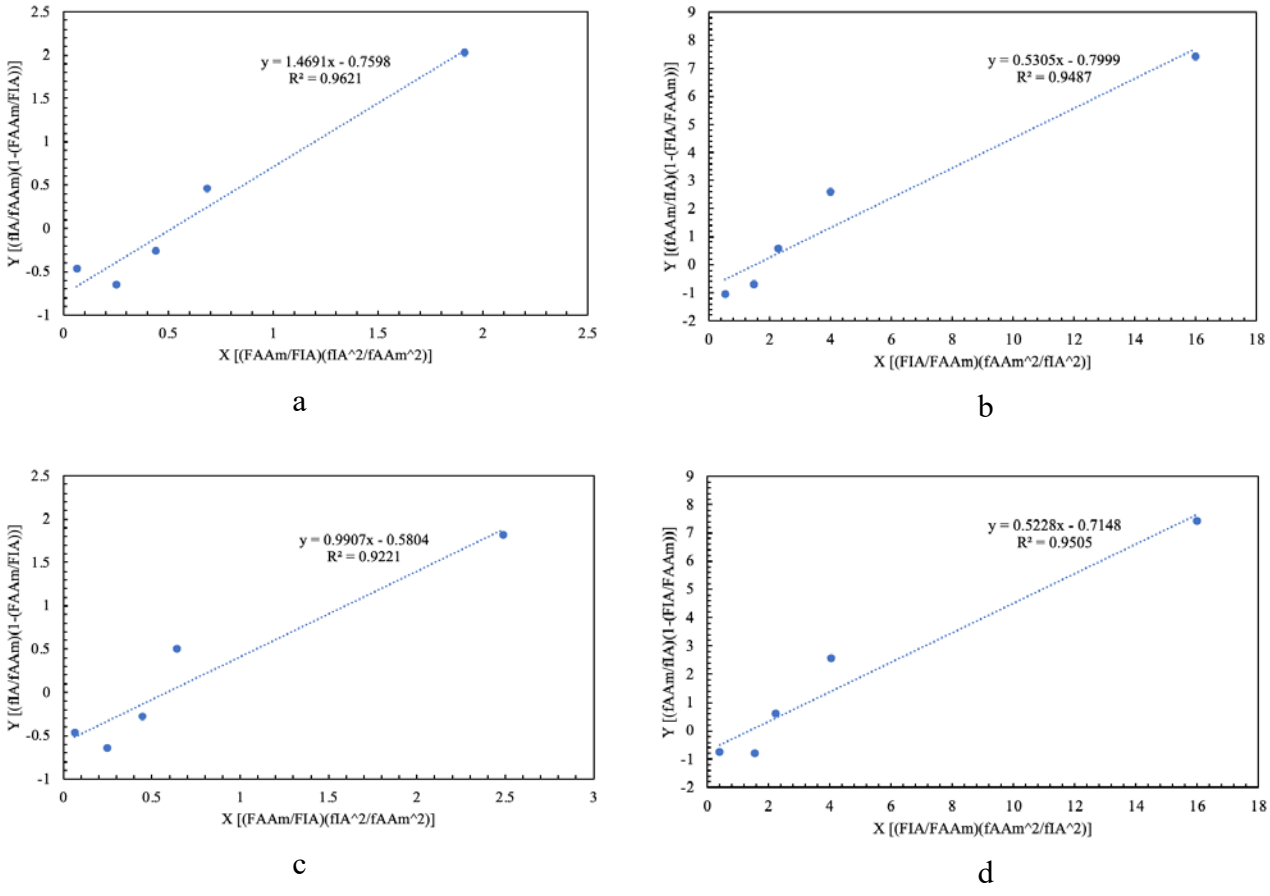

Figure 3.2: Fineman-Ross Results with a Comparison of Different Monomer 1 (m_1) Definitions [Conductometric Study with (a) m_1=IA and (b) m_1=AAm; Potentiometric Study with (c) m_1=IA and (d) m_1=AAm]

The reactivity ratios that were calculated and reported in Table 3.2 are the ones with monomer 1 as itaconic acid. These results best match the reactivity ratios published by Erbil et al., however

they did not explicitly define monomer 1 as itaconic acid. All four sets of calculated reactivity ratios can be found in Table 3.3.

Table 3.3: Reactivity Ratio Estimates Calculated using the Fineman-Ross Model

	Conductometric Titration [3]		Potentiometric Titration [4]	
	r_{IA}	r_{AAm}	r_{IA}	r_{AAm}
m_1=IA	1.4691	0.7598	0.9907	0.5804
m_1=AAm	0.7999	0.5305	0.7148	0.5228

The biggest difference when the definition of monomer 1 varies can be seen in the itaconic acid reactivity ratio for the conductometric titration data. It is almost halved when acrylamide is chosen as monomer 1 which would change the predicted behaviour of how each monomer is being incorporated into the copolymer as well as impacting the predicted microstructure of the copolymer. A $r_{IA} < 1$ would mean that both comonomers would have a higher affinity for cross-propagation and would predict copolymers with more of an alternating structure, rather than the 'blocky' structure that one would expect with $r_{IA} > 1$.

The next estimation technique that was investigated was the Kelen-Tüdös method. As explained in Section 2.5.2, this method uses a correction factor that helps make the experimental data points equally weighted. This is observed in Figure 3.3, where the data points are spaced equally along the x-axis. This helps to solve one of the issues of the Fineman-Ross approach, where some experimental data points are weighted more heavily which can skew the reactivity ratio estimation.

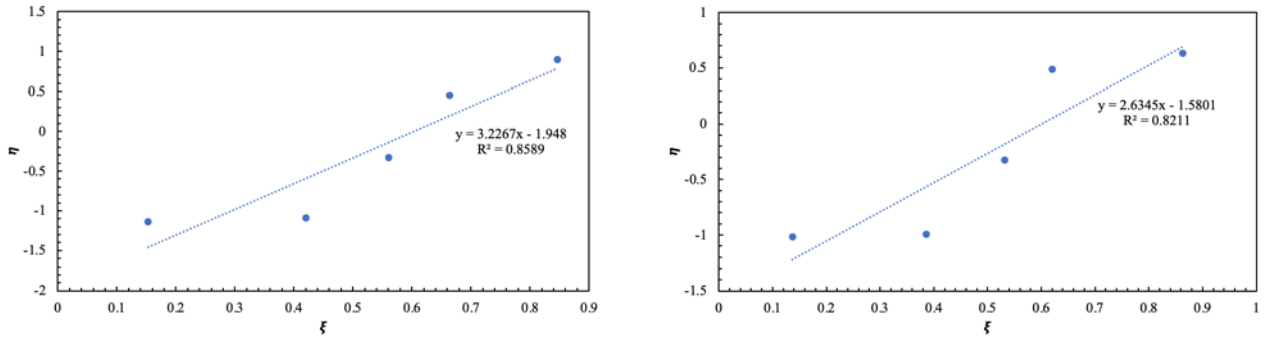

a b

Figure 3.3: Kelen-Tüdös Results using (a) Conductometric Data and (b) Potentiometric Data

The recalculated reactivity ratios were determined to be r_{IA}=1.2787 and r_{AAm}=0.6753 using the conductometric data, and r_{IA}=1.0544 and r_{AAm}=0.6263 using the potentiometric data. These values are very close to the values reported by Erbil et al. [3, 4]. However, the experimental data in Figure 3.3 are quite non-linear, and fitting a linear estimation model is inherently flawed.

The final linear estimation model that was evaluated was the extended Kelen-Tüdös model, as shown in Figure 3.4. This model takes the previous Kelen- Tüdös model a step further by incorporating the conversion into the estimation equation (recall Section 2.5.2). The results from this model were r_{IA}=1.361 and r_{AAm}=0.5654 using the conductometric data, and r_{IA}=1.0203 and r_{AAm}=0.5915 using the potentiometric data. These results are, like the Kelen- Tüdös method, very close to the results reported by Erbil et al. [3, 4]. Similarly, to both the Fineman-Ross and Kelen-Tüdös approaches, the model does not provide a good fit for the experimental data, which invites speculation about the accuracy of these reactivity ratio estimation results.

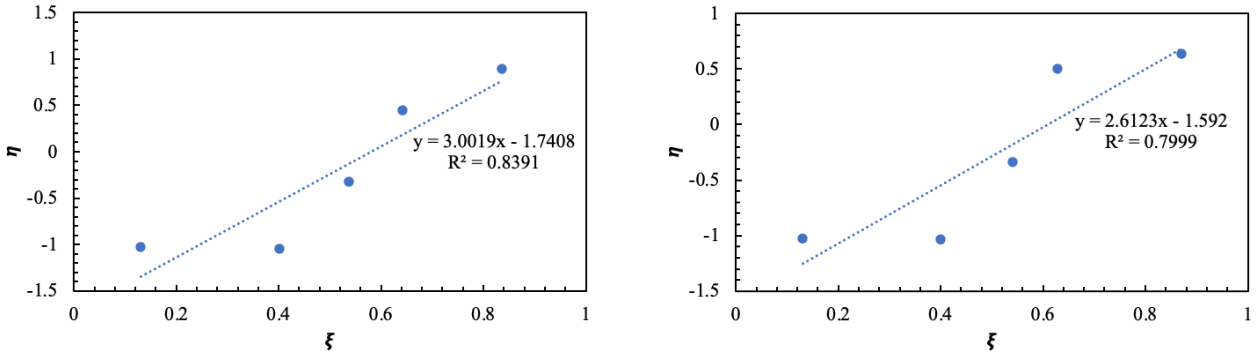

a b

Figure 3.4: Extended Kelen-Tüdös Results for the (a) Conductometric Data and (b) Potentiometric Data

The two Kelen-Tüdös models produced very similar reactivity ratios within the individual studies (that is, minor differences were seen between the Kelen-Tüdös and extended Kelen-Tüdös estimation results for a given experimental data set). This suggests that the extra computational steps of considering the conversion had little impact on the estimation results for this copolymer system. This could be because the majority of the data used in this study were kept below 10% conversion, and the main advantage of the extended Kelen-Tüdös method is that it can accommodate conversions up to 40%. Since the high conversion analysis was unnecessary in the current study, the results of the two estimation techniques were similar.

Overall, all four linear models outlined above provided similar reactivity ratios within the potentiometric titration study, except for the Mayo-Lewis method of intersections which had fairly larger estimates for both reactivity ratios. Within the conductometric titration study, there was a bit more variation within the reactivity ratios with the Kelen-Tüdös and extended Kelen-Tüdös being similar. For the most part, the itaconic acid reactivity ratios changed the most between the two studies with conductometric titration data resulting in higher reactivity ratio estimations. This

was not expected since the copolymer compositions reported for both studies were nearly identical except for runs 4 and 5 which were just slightly different.

Finally, EVM was used to compare reactivity ratio estimation results to what was re-estimated using the experimental compositions reported by Erbil et al. [3, 4]. EVM was used to obtain multiple reactivity ratio estimates, to compare the two literature studies and to compare the instantaneous and cumulative copolymerization models within EVM; the results are reported in Table 3.4. The first two rows of reactivity ratio estimates in Table 3.4 are the EVM results using data from a single respective study, and the final row uses both data sets within the same EVM estimation. The Kelen-Tüdös results from the respective study were used as the initial estimates, following the method outlined by Hagiopol [43]. For estimation using the combined data sets, the Kelen-Tüdös results from the conductometric study were used as the initial estimates, since within the conductometric study it was concluded that the compositions determined through conductometric titration were more reliable than those determined through potentiometric titration [3].

Table 3.4: EVM Reactivity Ratio Estimate Comparisons between the Instantaneous and Cumulative Models

	Instantaneous Model		Cumulative Model	
	r_{IA}	r_{AAm}	r_{IA}	r_{AAm}
Conductometric Titration	1.0731	0.6409	1.0623	0.6234
Potentiometric Titration	1.0054	0.6273	0.9914	0.6091
Both Data Sets	1.0395	0.6341	1.0271	0.6163

The EVM estimates are reasonably close to the results reported by Erbil et al. [3, 4], particularly to the Kelen-Tüdös and extended Kelen-Tüdös estimates in the potentiometric titration study. Figures 3.5 and 3.6 compare the EVM results from the combined data for the instantaneous and cumulative models, respectively, against the reactivity ratios re-estimated using the data produced by Erbil et al. [3, 4]. These results are more trustworthy since EVM is designed to be more statically robust and to account for error in both the independent (comonomer feed composition) and the dependent (copolymer composition) variables. However, EVM is limited by the quality of the data provided.

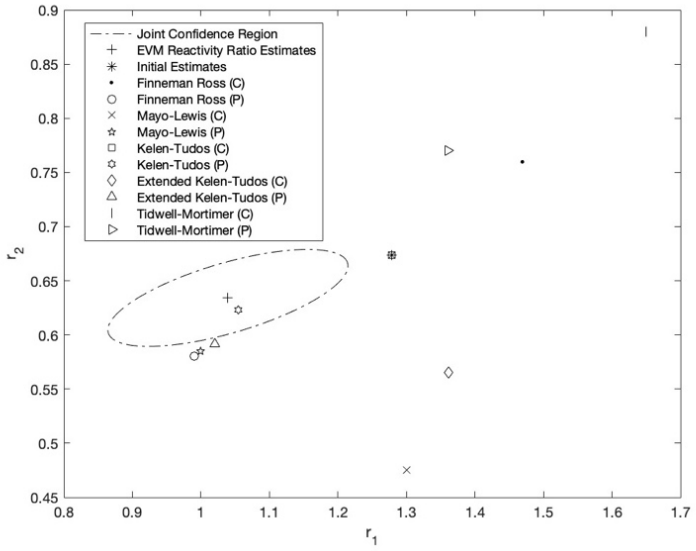

Figure 3.5: Instantaneous EVM Results using Data from both the Conductometric and Potentiometric Studies by Erbil et al. [3, 4] and Comparison to Traditional Techniques; $r_1=r_{IA}$ and $r_2=r_{AAm}$

Both the instantaneous and cumulative models provided similar estimation results. It is interesting to note that the 95% joint confidence region (JCR) encompasses more of the re-estimated reactivity ratios with the cumulative model (Figure 3.6) in comparison to the instantaneous model (Figure 3.5).

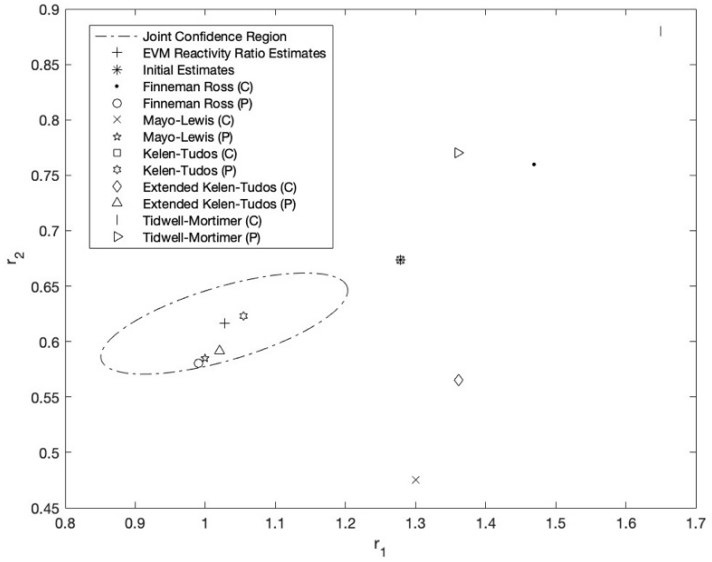

Figure 3.6: Cumulative EVM Results using Data from both the Conductometric and Potentiometric Studies by Erbil et al. [3, 4] and Comparison to Traditional Estimation Techniques; $r_1=r_{IA}$ and $r_2=r_{AAm}$

As shown in Figures 3.7 and 3.8, the instantaneous copolymer composition equation (recall Equation 2.8) was used to evaluate the accuracy of the reactivity ratio estimates obtained from different estimation methods, in terms of predicting the instantaneous composition relative to the actual experimental values.

The results of Figures 3.7 and 3.8 indicate that the experimental data do not seem to follow any of the model predictions. It is also interesting to note that several of the predictions are quite similar, which was not initially expected. Within the conductometric model predictions, there are slight differences between the different estimation models, however the potentiometric model predictions are almost identical. This is somewhat surprising since, as stated previously, the only two data points that are slightly different between the two studies are the copolymer compositions for runs 4 and 5, which resulted in r_{IA} being higher in the conductometric study.

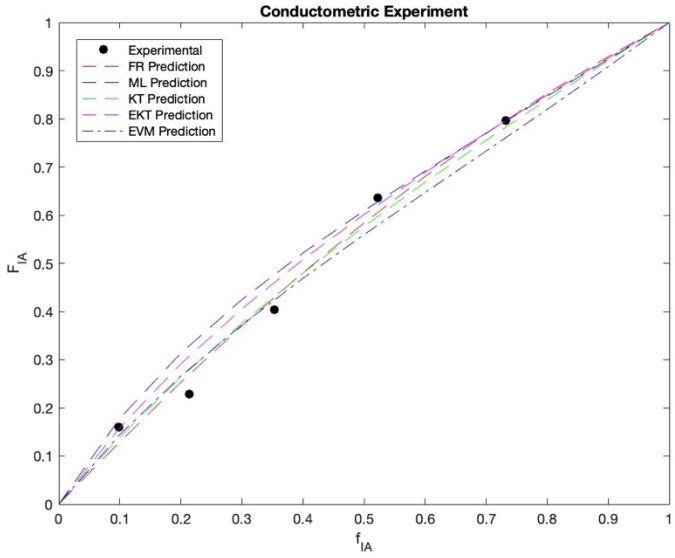

Figure 3.7: ICC Model Prediction versus Experimental Results for Conductometric Titration Study

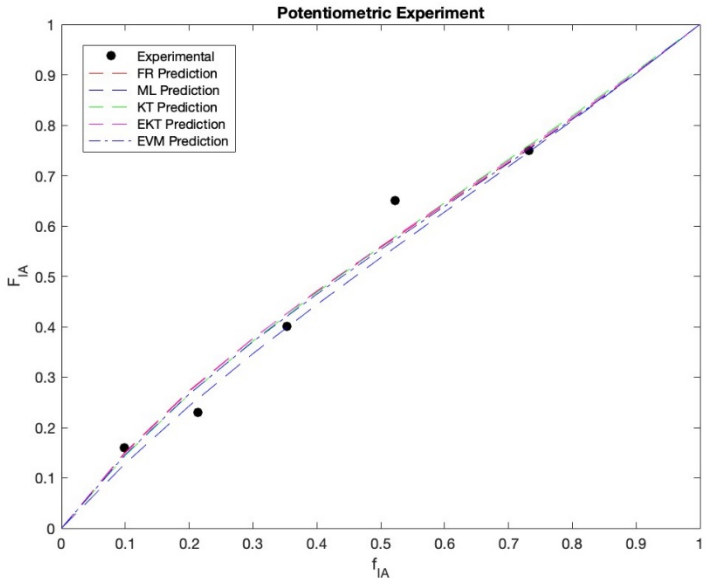

Figure 3.8: ICC Model Prediction versus Experimental Results for Potentiometric Titration Study

These studies reviewed in this chapter, published by Erbil et al. [3, 4], seem to be the only two kinetic studies evaluating the copolymerization of itaconic acid and acrylamide. Much of the

research performed on this copolymer system has been focused on hydrogel applications [39, 40, 41]. There is still very little known about the copolymerization kinetics of IA/AAm copolymers, and part of the motivation for the current study is to better understand the system and to provide reliable reactivity ratio estimates.

Chapter 4. Experimental Materials and Methods

4.1 Materials

The monomers acrylamide (AAm, 99% purity) and itaconic acid (IA, 99% purity) were purchased from Sigma-Aldrich, and both were used as received. The initiator, potassium persulfate (KPS, 99% purity), and inhibitor, hydroquinone (HQ, 99% purity) were also purchased from Sigma-Aldrich. The commercial polymers were provided by the Centre for Water Resource Studies (Dr. Amina Stoddart) at Dalhousie University. The solvents, HPLC grade water and methanol, were used as received from Sigma-Aldrich. Acetone was used as received from Dalhousie Chemistry Stores. Nitrogen gas (ultra-high purity) was used for degassing and was purchased from Linde.

The gel permeation chromatography (GPC) buffer solution was made using sodium nitrate (98% purity), sodium phosphate monobasic monohydrate (98% purity), and sodium phosphate dibasic heptahydrate (98% purity), which were purchased from Sigma-Aldrich. The GPC was calibrated using polyethylene oxide standards purchased from Agilent, and validated using poly(acrylamide-co-acrylic acid) purchased from Sigma-Aldrich. The elemental analysis system was calibrated using acetanilide (99.5%) purchased from Sigma-Aldrich and sulfanilamide purchased from Elementar.

4.2 Copolymer Synthesis

Aqueous monomer stock solutions with a total monomer concentration of 1 M were prepared at a variety of feed compositions (i.e., different comonomer ratios) of IA and AAm. These feed compositions are not provided here, as they will be described in detail within the experimental design in Section 5.1. For higher concentrations of IA, the volumetric flask with the monomer

stock solution was set on a stir plate with a stir bar to promote dissolution of the IA. These monomer stock solutions were stored in the fridge at approximately 6°C until they were used for synthesis.

For a five-sample polymerization (where each sample is approximately 20 mL), a 100 mL pre-polymerization solution was prepared. This included 90 mL of the monomer stock solution and 10 mL of HPLC grade water with approximately 64 mg of KPS. This made the total monomer concentration 0.9 M for the actual polymerization. The pH of the pre-polymer solution was not adjusted but was measured and recorded. The pH ranged from 2.06 to 2.45 for the highest to the lowest IA concentrations, respectively. This pH range is acceptable, as above pH 3.8 one of the carboxyl groups of itaconic acid becomes deprotonated [27], however below pH 2 acrylamide becomes protonated which causes its reactivity to decrease [46].

The 0.9 M pre-polymer solution was transferred to a round bottom flask, sealed with a rubber septum, and degassed with nitrogen gas for 2 hours. This ensured that there was no oxygen present in the flask, as oxygen can inhibit free radical polymerization by reacting with the active radicals and generating dead chain ends [47]. After degassing, 20 mL of solution was transferred to each sealed reaction vial using the cannula transfer method [48]. The vials were then sealed with parafilm, placed in a water bath (VWR 12L Shaking Bath) at 50°C and shaken at 100 rpm to initiate the polymerization reaction. The vials were removed at desired time intervals in an effort to better understand polymer characteristics as a function of conversion. Once the vials were removed from the water bath, they were placed in an ice bath and injected with approximately 0.5 mL of 0.2 M hydroquinone solution to terminate the reaction.

The polymer samples were isolated by precipitating the contents of the vials in an excess of acetone. The polymer samples were then filtered using pre-weighed Whatman Grade 40 ashless filter paper, and the samples were left in the fume hood overnight so that any remaining acetone would evaporate prior to being placed in the vacuum oven. The samples were then transferred to the vacuum oven at 50°C for approximately one week to remove any remaining water from the polymer. The drying time was determined based on the time it took for mass measurements to stabilize.

4.3 Characterization Methods

The mass conversion of the polymer samples was determined through gravimetry. This was done by comparing the weight of the final dried polymer sample to the weight of monomer initially in the vial. The conversion can be calculated using Equation 4.1.

$$X_w = \frac{mass\ of\ polymer}{initial\ mass\ of\ monomer} \tag{4.1}$$

The dried polymer samples were then crushed using a mortar and pestle and stored for further characterization.

4.3.1 Elemental Analysis

Elemental analysis (Elementar Unicube CHNS) was used to determine the cumulative copolymer composition of commercially available and in-house synthesized materials. The elemental analyzer was calibrated using 5 runs; 2 blanks to burn off anything left within the equipment and

3 runs with sulfanilamide. 2 mg of solid polymer sample was measured into an aluminum weigh boat, which was carefully folded to completely enclose the polymer sample within the aluminum. The weigh boat was placed within a sample carousel where it was dropped into a 1150°C furnace, and the material was subsequently combusted and reduced to N_2, CO_2, H_2O, and SO_2 gases. The mass percents of hydrogen, carbon, nitrogen, and sulfur in the samples were then determined based on the known mass of the sample.

Since acrylamide has nitrogen present in its structure and itaconic acid does not, the amount of nitrogen measured can be used to calculate the amount of acrylamide present in the copolymer. Once the amount of carbon contained in the acrylamide is known, the remaining carbon can be used to calculate the amount of itaconic acid present (sample calculations can be found in Appendix A). Hydrogen is not used in the calculation of the composition, since the polymer samples may absorb moisture from the atmosphere given the hydrophilicity of the polymer samples.

4.3.2 Gel Permeation Chromatography

An aqueous gel permeation chromatography (GPC) system with triple detection (Agilent 1260 Infinity II) was used to determine the weight-average molecular weights ($\overline{M_w}$) and molecular weight distributions (MWD) of all samples. GPC is a form of size exclusion chromatography which uses refractive index, light scattering, and viscometry to calculate molecular weight averages and molecular weight distribution. The buffer solution used for the mobile phase was 0.2 M sodium nitrate, 0.01 M sodium phosphate monobasic monohydrate, and 0.01 M sodium phosphate dibasic heptahydrate in HPLC water. The system includes two PL aqua gel-OH columns

(8 μm particle size, 300 by 7.5 mm) as well as a PL aqua gel-OH guard column. The system was calibrated with 6 polyethylene oxide standards with peak molecular weights ranging from 8500 to $1.5 \cdot 10^6$ g/mol. The calibration was validated using a commercial poly(acrylamide-co-acrylic acid) with a known $\overline{M_w}$ of $5.2 \cdot 10^5$ g/mol.

The samples were run at a temperature of 40 °C, a flow rate of 1 mL/min, an injection volume of 100 μL, and all three detectors had the same sampling rate of 1 Hz. The itaconic acid/acrylamide copolymer samples were prepared at a concentration of 1 mg/mL and the commercial samples were prepared at a concentration of 0.5 mg/mL, both in an aqueous buffer solution. The samples were dissolved with the help of a stir bar at 500 rpm for 2 hours for the itaconic acid/acrylamide samples and for up to 4 hours for the commercial samples. All samples were filtered using a 0.45 μm PTFE filter prior to being injected into the GPC system.

4.3.3 Zeta Potential

The samples' zeta potential was determined using a Malvern Zetasizer Nano ZS with gold electrode cells. The zeta potential of a material represents the net surface charge, or charge density, and can be a measure of how strongly a flocculant will attract contaminants. The polymer samples were prepared in HPLC grade water at a concentration of 1.5 mg/mL for the itaconic acid/acrylamide polymers and 2 mg/mL for the commercial polymer flocculants. The samples were run in triplicate, with the software calculating the standard deviation of the three runs.

Chapter 5. Preliminary Experiments

The goal of the preliminary experiments was to gain an understanding of the experimental limitations and kinetic properties of the poly (itaconic acid-co-acrylamide) system. To the best of our knowledge, there are only two published kinetic studies [3, 4] for this specific copolymer system. These two studies, performed by the same research group in 1999 and 2000, used two separate titration methods for determining copolymer composition and five separate methods for estimating reactivity ratios. However, as discussed in Chapter 3, some questions remain about the quality of the data presented within those studies. Therefore, the preliminary experimental stage in the current work aimed to update these findings using more efficient and reliable experimental methods and statistically correct reactivity ratio estimation techniques such as the error-in-variables model.

5.1 Design of Experiments

Since it has been over two decades since the studies by Erbil et al. [3, 4] were published, and there have been many advances in research and technology since then, new experimental data for this copolymer system was collected for the current study.

To guide the preliminary experiments, a design of experiments using the error-in-variables model (EVM) was conducted based on work by Kazemi et al. [49]. The design of experiments identified two feed compositions that would provide the most information for reactivity ratio estimation: $f_{1,1,0} = 0.10$ and $f_{1,2,0} = 0.54$, where monomer 1 is itaconic acid. As previously stated in Section 4.2, the total monomer concentration was kept constant at 0.9 M, but the proportion of the two comonomers was varied. The $f_{IA,0}$=0.1 feed composition (with the balance acrylamide) successfully polymerized; however preliminary experiments determined that the feed composition

of $f_{IA,0}$=0.54 itaconic acid did not produce solid polymer within 48 hours. This could be due to a number of factors, but it is likely that since free-radical polymerization of itaconic acid is a fairly slow reaction, the high mole fraction is increasing the polymerization time past a reasonable duration for this project [27]. This observation aligns with other studies, such as a study on the homopolymerization of itaconic acid, that required moderately larger amounts of initiator to achieve successful polymerizations within 17 hours [50]. Cummings et al. [24] also reported that they kept the feed composition of itaconic acid below 25 mol% due to the poor solubility of itaconic acid and the reaction dependence on pH.

Since the $f_{IA,0}$=0.54 feed composition failed to polymerize within 24 hours, a second run was done at the same feed composition that was prolonged to 96 hours, and still no solid polymer was observed. To troubleshoot this result, the isolation step was evaluated; namely, the suitability of an acetone non-solvent for itaconic acid isolation was investigated. A comparison was performed to evaluate methanol and acetone as non-solvents, and acetone performed better based on observed precipitate quality.

5.2 Selection of Key Variables

The key variables that were selected for this study were the monomer concentration, the feed composition, and the initiator concentration. These variables were expected to have the strongest impact on the characteristics chosen to evaluate the synthesized polymers (molecular weight averages, copolymer composition, and zeta potential; to be described further in Section 5.4). The goal of this design stage is to develop relationships between these key synthesis variables (which

can be tailored or optimized) and the resulting copolymer characteristics. These results will also contribute to a better understanding of the copolymer system.

5.3 Synthesis of Polymer Product

Following the design framework (recall Section 2.1), the novel itaconic acid and acrylamide copolymers were synthesized according to the design of experiments outlined in Section 5.1. For brevity, the synthesis results will be provided in Section 5.4.2, along with the polymer characterization results.

5.4 Characterization of Key Aspects of Polymer Product

The three characteristics that were considered for these polymer products were cumulative copolymer composition, molecular weight averages, and zeta potential. The cumulative copolymer composition was chosen as a key characteristic since it is a crucial consideration for determining reactivity ratio estimates. As discussed in Section 2.3.2, the copolymer composition can also impact the flocculation ability, depending on how much of the charged comonomer is incorporated into the copolymer and how it is incorporated (i.e., the microstructure of the copolymer). The molecular weight averages and the zeta potential were chosen as the other key characteristics as they are expected to have an impact on the size of the flocs that can be formed and the efficiency of the polymer as a flocculant.

5.4.1 Characterization of Commercial Flocculants

Three commercial anionic flocculants from different manufacturers (obtained from Dr. Amina Stoddart at the Centre for Water Resources Studies, Dalhousie University) were characterized using the methods described in Sections 4.3.1-4.3.3. This preliminary investigation was performed to provide benchmark values for the novel flocculants being synthesized in this project. The commercial flocculants have been labeled A, B, and C for confidentiality reasons.

The first property that was determined was the cumulative copolymer composition, which was calculated using elemental analysis (EA) data. EA measures the mass percent of hydrogen, carbon, nitrogen, and sulfur present in each sample. The mass percent of sulfur was found to be negligible; it was within the noise of the elemental analysis equipment and was therefore excluded from the empirical formula. The remaining mass percents of carbon, hydrogen, and nitrogen did not sum to 100%, so the remainder was assumed to be oxygen (sample calculations are presented in Appendix A). This assumption was based on the fact that oxygen is present in many monomers known to be used in industrial polymer flocculants, including acrylamide and acrylic acid. As seen in Table 5.1, all three commercial samples had similar empirical formulas. This suggests that all three samples may have been synthesized using the same comonomers. If one were to make an additional assumption that the commercial flocculants were produced from acrylamide and acrylic acid, the composition of each sample could be calculated. Samples A and C were found to have similar compositions of 22% acrylic acid and 19% acrylic acid, respectively. Sample B also had a composition containing more acrylamide than acrylic acid, but had a lower percentage of acrylic acid than the other samples.

Table 5.1: Approximate Empirical Formulas and Proposed Compositions for Commercial Polymer Flocculants

Sample	Approximate Empirical Formula	Composition (mol %)
A	$C_4H_7NO_3$	22% Acrylic Acid, 78% Acrylamide
B	$C_4H_7NO_3$	14% Acrylic Acid, 86% Acrylamide
C	$C_4H_7NO_3$	19% Acrylic Acid, 81% Acrylamide

Table 5.1 demonstrates that the commercially available polymer flocculants all have similar compositions and identical (approximate) empirical formulas. All three samples were found to be acrylamide-rich with approximately 15-20 mol% of the charged comonomer. This suggests that there is room for innovation within the wastewater treatment industry, and there is significant potential to develop new materials for this application. These results also provide a benchmark for the current project of targeting acrylamide-rich compositions (~80 mol%) for designed polymer flocculants.

In parallel, the molecular weights provided by the manufacturers were confirmed using gel permeation chromatography (GPC). As stated previously, it is unclear which molecular weight average is provided by the manufacturer. As seen in Table 5.2, the weight-average molecular weights ($\overline{M_w}$) determined by GPC were of the same order of magnitude as the values reported by the commercial flocculant manufacturers. However, it is important to note that Sample A's molecular weight was not provided by the manufacturer. This is a good example that not all flocculant characteristics are provided by the manufacturers, and it is important to characterize representative commercial flocculants so that those characteristics can act as benchmark values during the design of novel polymer flocculants. All three commercial samples had $\overline{M_w}$ around 10^7

g/mol, which is aligned with the application requirements (namely, high molecular weight polymers).

An experimental limitation is that molecular weights of this magnitude can be difficult to accurately measure, since the GPC can only be calibrated up to $1.5 \cdot 10^6$ g/mol. However, this is not just a limitation for this study, but a limitation of high molecular weight characterization of water-soluble polymers in general. This means that manufacturers supplying molecular weight data are subject to the same limitations as reported in the current study, especially when evaluating high molecular weight polymers.

Table 5.2: Molecular Weights of the Commercial Polymer Flocculants

Sample	$\overline{M_w}$ (g/mol)	Polydispersity Index (PDI)	Manufacturer Provided MW (g/mol)
A	$9.51 \cdot 10^6$	1.006	-
B	$13.48 \cdot 10^6$	1.008	$18.50 \cdot 10^6$
C	$11.97 \cdot 10^6$	1.003	$19.06 \cdot 10^6$

It is also interesting to note here that the polydispersity index (PDI) (measured via GPC) for these commercial polymers is very small. As was described in Section 2.3.1, narrow molecular weight distributions (low PDI) are desired for polymer flocculants, since the majority of the polymer chains within the sample will be long chain, high molecular weight polymers and will be able to participate in the flocculation mechanisms. This allows for smaller dosages of flocculants to be used. However, these PDI values further demonstrate the limitations of the GPC system as a PDI

of 1 would mean that there is virtually no dispersity within the sample and that is not physically possible.

The final step was to determine the zeta potential for each commercial flocculant, which is reported in Table 5.3. All three samples had similar zeta potentials around -100 mV. This supports the results reported in Table 5.1; since zeta potential measures the net surface charge of a polymer, having samples with similar zeta potentials suggests that the commercial polymers have similar proportions of the charged comonomer incorporated into the copolymer. Each sample was analyzed in triplicate, and the average is reported in Table 5.3.

Table 5.3: Zeta Potentials of Commercial Polymer Flocculants

Sample	Zeta Potential (mV)	Std. Dev. (mV)
A	-106.00	+/- 0
B	-100.75	+/- 4.25
C	-123.50	+/- 0.50

As shown in Table 5.3, Sample B had the lowest zeta potential of the three commercial flocculants. Interestingly, Sample B also had the lowest proportion of acrylic acid, estimated at just 14% (recall Table 5.1). As such, there may be a relationship between anionic comonomer incorporation and zeta potential. However, this trend is not observed for the remaining samples (A and C), which suggests that the relationship between the amount of the anionic comonomer and the zeta potential is not a straightforward correlation and that there may be other factors impacting the zeta potential. It is also interesting to note that the standard deviation for samples A and C are very low. These standard deviations were determined by the software after the analysis of each sample in triplicate.

5.4.2 Synthesis and Characterization of Itaconic Acid/Acrylamide Copolymers

Since $f_{IA,0}$ =0.54 did not polymerize (as reported in Section 5.1), the next synthesis step was to conduct a study comparing different feed compositions and determining the IA concentration threshold for this synthesis approach. This is related to feed composition being a key variable for gaining a better understanding of this copolymer system. Five feed compositions were chosen between 10 mol% IA and 54 mol% itaconic acid: 10 mol% IA, 20 mol% IA, 30 mol% IA, 40 mol% IA, and 50 mol% IA. These were all initially synthesized with 2 replicates to verify results. While the lower concentrations of itaconic acid polymerized successfully, polymerization became less effective at higher itaconic acid concentrations; a summary of observations is provided in Table 5.4.

Table 5.4: Qualitative Observations from Preliminary IA/AAm Copolymerization Experiments

$f_{IA,0}$	**Synthesis Results**
0.1	Polymerized successfully
0.2	Polymerized successfully
0.3	Polymerized with some experimental limitations
0.4	Did not polymerize within 96 hours
0.5	

The preliminary conversion vs. time results from $f_{IA,0}$ = 0.1 and 0.2 are shown in Figures 5.1 and 5.2, respectively. It is interesting to note here that as more itaconic acid is included in the feed, the reaction time increases, and it takes longer for the 20 mol% IA system to achieve the same level of conversion as the 10 mol% IA system. This could be because acrylamide is known to be the

more reactive monomer, so as the amount of acrylamide decreases it makes sense that the rate of polymerization decreases.

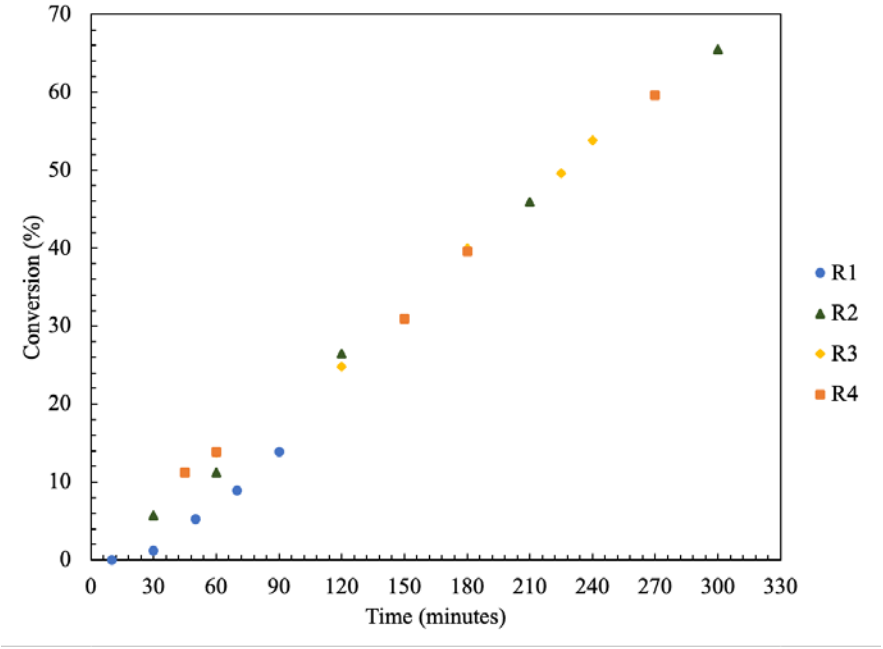

Figure 5.1: Conversion as a Function of Time for the Feed Compositions of $f_{IA,0} = 0.1$

The conversion vs. time results for $f_{IA,0} = 0.1$ show that the data are reproducible, especially after 15% conversion. The variability in the data below 15% conversion further demonstrates that linear methods are not appropriate for reactivity ratio estimation; even within the same system, the results are less predictable below 10% conversion. Since linear methods require low conversion data to avoid composition drift, this is an obvious experimental limitation. These preliminary experiments were kept within 5 hours to ensure that experiments took a reasonable length of time. Initially, only 2 replicates were completed for each of the feed compositions, however 2 additional replicates were added for $f_{IA,0} = 0.1$ to verify the higher conversion data and to fill in the experimental gaps to better understand the system.

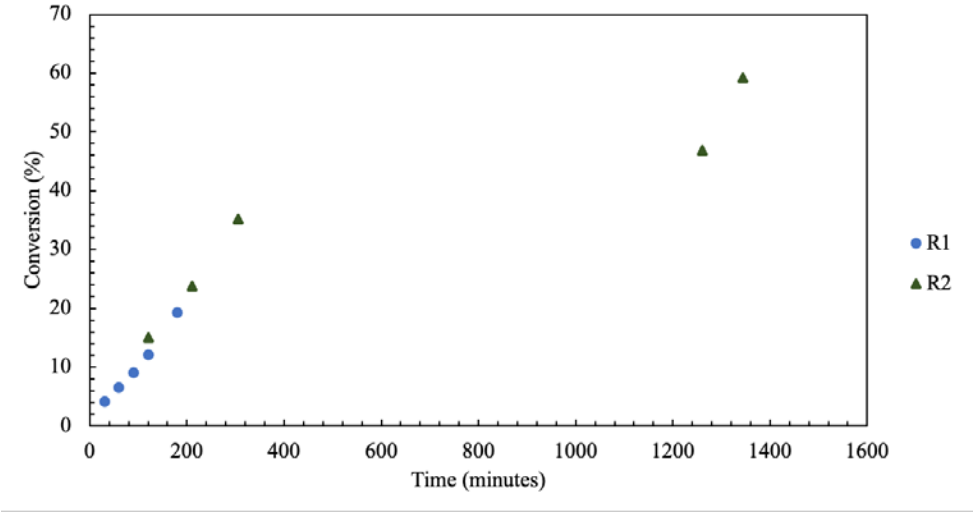

Figure 5.2: Conversion as a Function of Time for the Feed Composition of $f_{IA,0} = 0.2$

The first experiment using 20 mol% IA (R1 in Figure 5.2) was performed for 3 hours, however only a 20% mass conversion was achieved. Therefore, the replicate run (R2 in Figure 5.2) was extended to 22.5 hours, where a 59.3 mass % conversion was achieved. This suggests that for the 20 mol% IA formulation to achieve approximately the same level of conversion as the 10 mol% IA formulation, it takes 18 additional hours of polymerization. This makes sense since acrylamide is known to be more reactive than itaconic acid, so as the amount of acrylamide in the feed is decreased, the polymerization rate would decrease as well. This ultimately increases the amount of time it will take to achieve the same level of conversion. Additionally, the trend observed in Figure 5.2 does not follow the strictly linear relationship that was seen in Figure 5.1 for $f_{IA,0} = 0.1$. The trajectory is especially inconsistent at the higher time points, which will be evaluated further in Chapter 6.

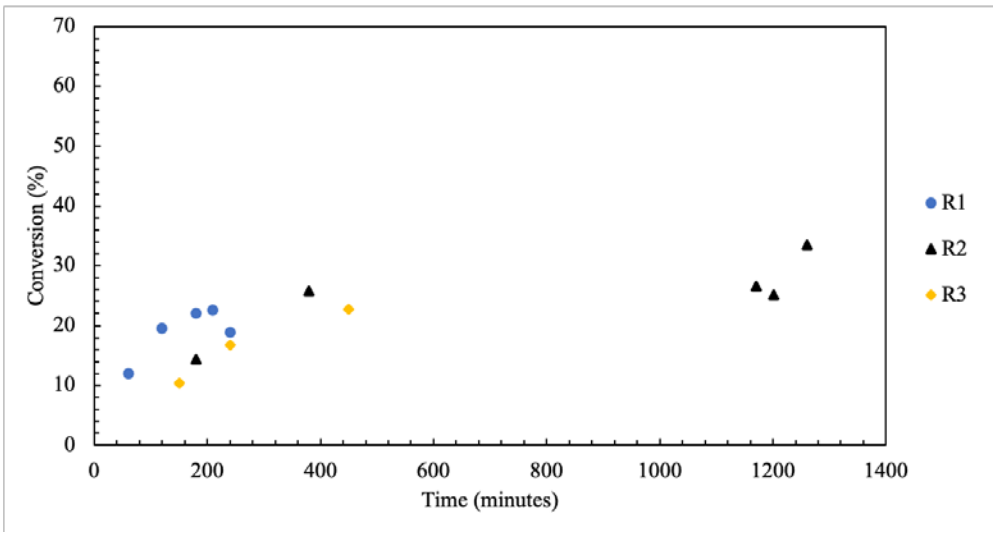

Figure 5.3: Conversion as a Function of Time for the Feed Composition of $f_{IA,0} = 0.3$

Figure 5.3 shows the conversion vs. time results for the polymerization of the 30 mol% IA formulation. The results showed poor reproducibility and there were issues observed with the isolation of the copolymer product. This could be because there was insufficient non-solvent (acetone) and too much water in this isolation process, causing some samples to remain partially dissolved. As such, two outlying data points were removed from R3, and isolation protocols were evaluated qualitatively. There was an additional replicate completed for this feed composition to validate the data, given the poor reproducibility of the first two runs.

The copolymers produced from the feed compositions of $f_{IA,0}$ = 0.1, 0.2 and 0.3 were then characterized using elemental analysis, gel permeation chromatography and zeta potential. Elemental analysis was used to determine the copolymer composition. This was done partially to confirm that itaconic acid was being incorporated into the copolymer as well as for reactivity ratio estimations. Itaconic acid incorporation was also verified using nuclear magnetic resonance (NMR) spectroscopy, which can be found in Appendix B. Given the experimental limitations

observed during synthesis, it was not possible to include higher itaconic acid feed composition data in reactivity ratio estimation; this may not provide as full a picture of the system compared to DOE-informed data collection. However, in a study by Cummings et al. [24] they were successfully able to estimate reactivity ratios for itaconic acid and acrylic acid copolymers under similar experimental limitations.

For a preliminary understanding of copolymer composition, both the cumulative copolymer compositions and the empirical formulas were calculated by averaging all of the sample measurements for each feed composition. This included 7 samples for the 10 mol% IA formulation with 1 sample characterization replicated, 9 samples for the 20 mol% IA formulation with 1 sample characterization replicated, and 3 samples for the 30 mol% IA formulation. The mass percents of carbon, hydrogen, nitrogen and sulfur that were measured for all of the sample runs are summarized in Table A.2 in Appendix A, with the copolymer compositions and empirical formulas in Table 5.5.

Table 5.5: Copolymer Compositions and Approximate Empirical Formulas from Elemental Analysis Results

Feed Composition ($f_{IA,0}$)	**Copolymer Composition (mol%)**	**Approximate Empirical Formula**
0.1	21% Itaconic Acid, 79% Acrylamide	$C_4H_8NO_2$
0.2	35% Itaconic Acid, 65% Acrylamide	$C_6H_{10}NO_4$
0.3	47% Itaconic Acid, 53% Acrylamide	$C_7H_{13}NO_6$

The copolymer composition was found by converting the mass percent into moles per 100 grams by dividing the mass percent by the molar mass for each element (C, H, N, S). This was then

converted into a mole ratio by dividing each element by the moles per 100 grams of nitrogen. Nitrogen was selected as the basis for calculations because acrylamide contains nitrogen and itaconic acid does not, therefore all of the nitrogen present must come from the acrylamide portion of the copolymer. As discussed in Section 4.3.1, once the nitrogen present is used to calculate the amount of acrylamide in the copolymer, the amount of carbon contained in the acrylamide is known, and the remaining carbon can be used to calculate the amount of itaconic acid present.

The empirical formula represents the relative amount of each element present in each copolymer sample. It should be noted that the elemental analysis equipment was set up to measure the amount of carbon, nitrogen, hydrogen, and sulfur. As described previously in Section 5.4.1, the amount of sulfur detected was deemed to be negligible since it was similar to the amount of sulfur present in the 'blank' runs measured prior to sample runs. It is also possible that any sulfur detected was due to leftover initiator (potassium persulfate) in the copolymer products. Therefore, sulfur was excluded from the empirical formulas for all samples. It should also be noted that oxygen was not one of the elements being measured in the elemental analyzer. Again, as described previously in Section 5.4.1, the mass percents of the measured elements did not sum to 100%. Since, in this case, the copolymer is only expected to contain itaconic acid and acrylamide, it was assumed that the remaining mass was due to the presence of oxygen within the comonomers. These empirical formulas are representative of the relative amount of each element in the copolymer compared to the amount of nitrogen, the actual chemical formula would be much larger. Sample calculations can be found in Appendix A.

The approximate empirical formula determined for the 10 mol% IA feed composition was most similar to the commercial flocculants, especially to sample A (recall Table 5.1). These two samples had similar proportions of the anionic monomer, with sample A containing 21% acrylic acid and the 10 mol% IA sample containing 22% itaconic acid. However, the 10 mol% itaconic acid has about 1.5 times the amount of oxygen, which makes sense since itaconic acid has an extra carboxylic acid group in its structure compared to acrylic acid. Again, this comparison relies on the assumption that sample A is a copolymer of acrylic acid and acrylamide, which cannot be confirmed.

The conversion and cumulative copolymer compositions were then used in the error-in-variables model (EVM), with both the instantaneous (Figure 5.4) and cumulative (Figure 5.5) copolymerization models, to calculate reactivity ratio estimates. The initial estimates used were the reactivity ratios determined using EVM in Chapter 3, which were calculated from the data published by Erbil et al. in 1999 and 2000 [3, 4]. These initial estimates were $r_1 = r_{IA} = 1.0271$ and $r_2 = r_{AAm} = 0.6163$, which are circled in red in Figure 5.4 and Figure 5.5.

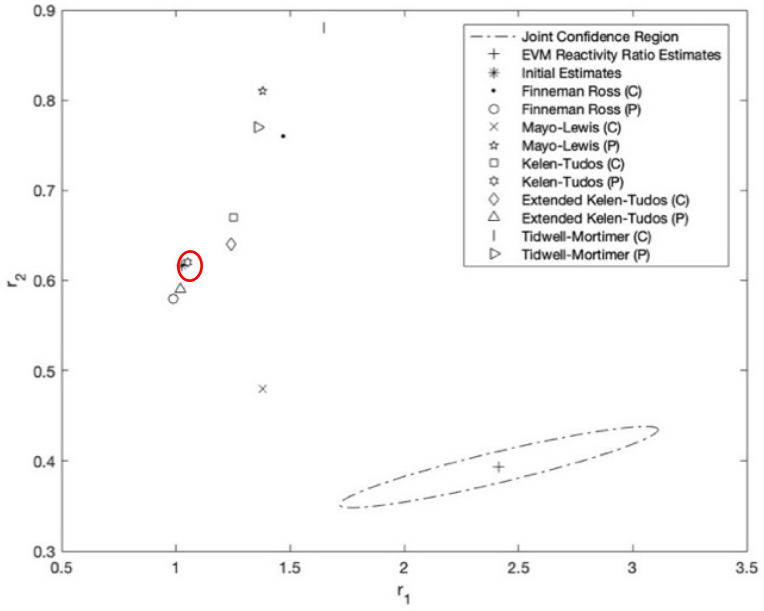

Figure 5.4: Instantaneous Reactivity Ratio Estimation Results using EVM (within the 95% dotted Joint Confidence Region) Compared to Reactivity Ratios Calculated using the Data from Erbil et al. [3, 4]

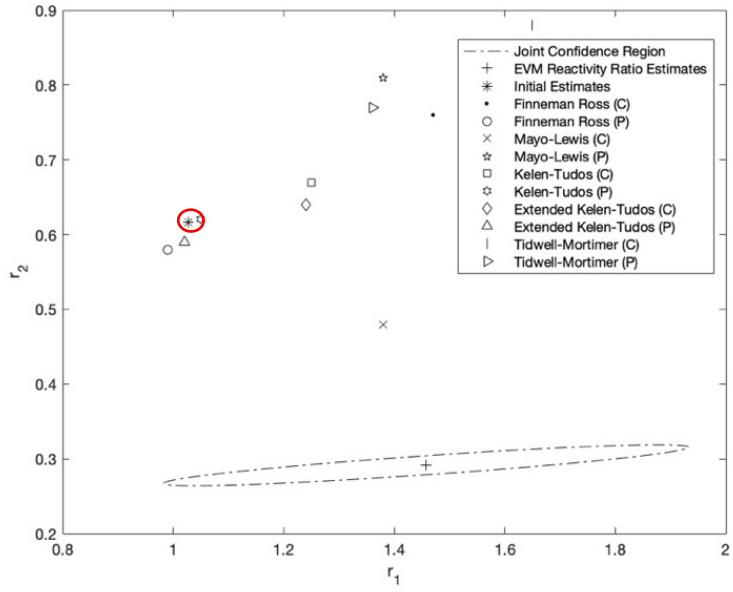

Figure 5.5: Cumulative Reactivity Ratio Estimates using EVM (within the 95% dotted Joint Confidence Region) Compared to Reactivity Ratios Calculated using the Data from Erbil et al. [3, 4]

The reactivity ratios calculated by the instantaneous EVM model using $f_{IA,0}$ =0.1 and 0.2 data with 3 replicates and 2 replicates respectively (R1, R2 and R3 from Figure 5.1, and R1 and R2 from Figure 5.2) were $r_1 = r_{IA}$ = 2.4136 and $r_2 = r_{AAm}$ = 0.3932. The reactivity ratios calculated by the cumulative EVM model using $f_{IA,0}$ =0.1 and 0.2 data, with the same replicates used for the instantaneous model, were $r_1 = r_{IA}$ =1.4577 and $r_2 = r_{AAm}$= 0.2914. This means that itaconic acid has a higher affinity for homo-propagation and acrylamide has a higher affinity for cross-propagation. Therefore, regardless of which monomer is in the terminal position of the growing radical chain, there will be a preference towards reacting with itaconic acid. The biggest difference between the instantaneous and cumulative models is the itaconic acid reactivity ratio estimate, r_{IA}. The trend is similar here to what was observed in Chapter 3, where $r_{IA} > 1$ and $r_{AAm} < 1$, however the instantaneous model results in an r_{IA} estimate that is nearly double that of the cumulative model. The instantaneous model only used the lower conversion experimental data (less than 15%), so there was a smaller data set to work with. Also, as seen in the conversion vs. time figures (Figures 5.1-5.3), the lower conversion data is much more variable than the higher conversion data, therefore the cumulative results are more trustworthy.

To validate the cumulative reactivity ratios, the experimentally determined cumulative copolymer compositions from $f_{IA,0}$=0.1 and $f_{IA,0}$=0.2 were plotted against conversion, and the Skeist equation was used to model the behaviour using the cumulative reactivity ratios (see Figure 5.6). The Skeist equation for cumulative copolymer composition is described in previous studies on copolymerization reactivity ratios using EVM [42, 45]. The experimental data from $f_{IA,0}$=0.3 was then used to see how closely the model prediction fits the data, as shown in Figure 5.7. This

comparison can be used for validation of the results since the $f_{IA,0}$=0.3 experimental composition data was not used for reactivity ratio estimation.

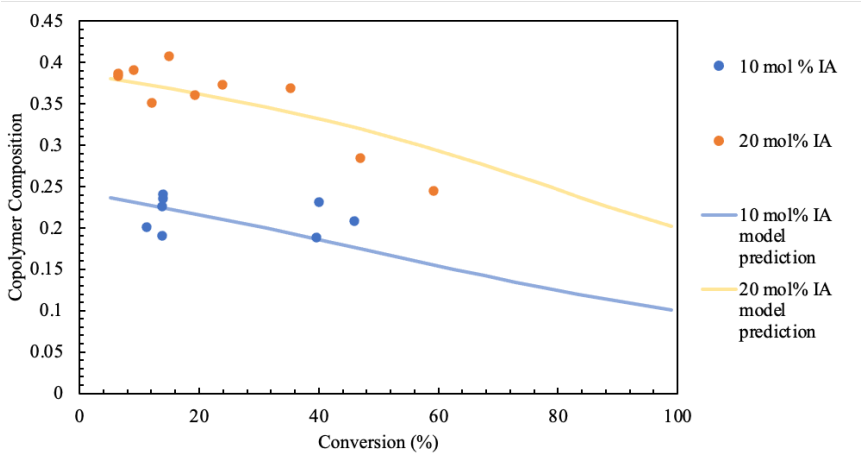

Figure 5.6: Cumulative Copolymer Composition versus Conversion with Model Predictions using the Skeist Equation

Figure 5.6 shows that the experimental data follow the general trends of the model predictions. The model predictions for both of the feed compositions show the composition drift that happens within this system (recall Section 2.5.2). The early conversion samples contain a higher amount of itaconic acid, and as the itaconic acid is consumed the acrylamide incorporation starts to increase, causing the overall fraction of itaconic acid in the copolymer to decrease.

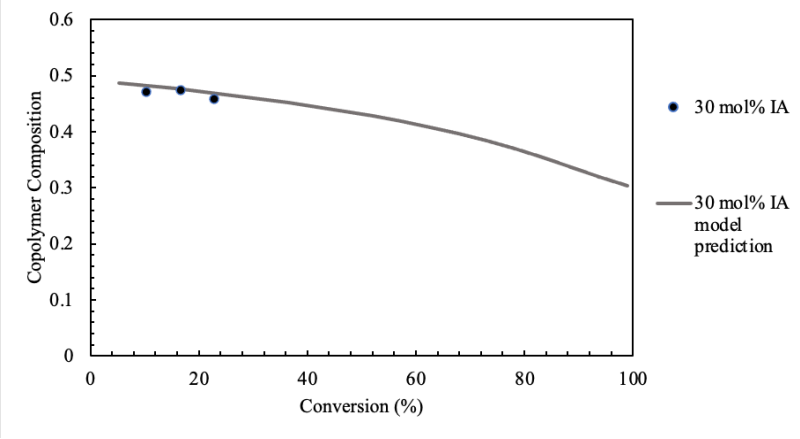

Figure 5.7: Reactivity Ratio Validation using $f_{IA,0}$ = 0.3 Experimental Data and Model Prediction using the Skeist Equation

Figure 5.7 confirms that the reactivity ratios are trustworthy for this copolymer system. Only three samples from the $f_{IA,0}$=0.3 experiments produced enough material to be tested using elemental analysis, which is why there are only three data points in Figure 5.7. These data points are in good agreement with the model prediction; however, it is not ideal that all of the available data to validate the reactivity ratios are at relatively low conversion.

Next, the $\overline{M_w}$ and molecular weight distribution were determined using gel permeation chromatography, outlined in Table 5.6. For the feed composition of $f_{IA,0}$ = 0.1, the poly(itaconic acid-co-acrylamide) sample reached a maximum $\overline{M_w}$ of 605 490 g/mol at a mass conversion of 53.5%. For the feed composition of $f_{IA,0}$ = 0.2, the poly(itaconic acid-co-acrylamide) sample reached a maximum $\overline{M_w}$ of 656 441 g/mol at a mass conversion of 61.1%. For the feed composition of $f_{IA,0}$ = 0.3, only a few solid polymer samples could be analyzed, since no solid polymer was isolated beyond a mass conversion of 25%. The sample synthesized from a $f_{IA,0}$ = 0.3 formulation that reached 14.3% conversion had a $\overline{M_w}$ of 193 216 g/mol.

Table 5.6: Maximum Observed Weight-Average Molecular Weights and Associated PDI of IA/AAm Copolymers

Feed Composition ($f_{IA,0}$)	**Conversion (%)**	**$\overline{M_w}$ (g/mol)**	**PDI**
0.1	53.8	605 490	1.216
0.2	61.1	656 441	2.854
0.3	14.3	193 216	1.385

The $\overline{M_w}$ of all samples were plotted against conversion for $f_{IA,0}$=0.1 and 0.2, which can be seen in Figures 5.8 and 5.9, respectively. These values are all single characterization measurements, as the focus was on getting as many samples tested as possible. It is interesting to note that the experimental data for $f_{IA,0}$=0.1 had PDI values below 2 all the way up to the maximum conversion of 65.5%. The experimental data for $f_{IA,0}$=0.2 had PDI values below 2 for the lower conversion data (below 25%) and all of the data at the higher conversions had PDI values between 2.5 and 3.

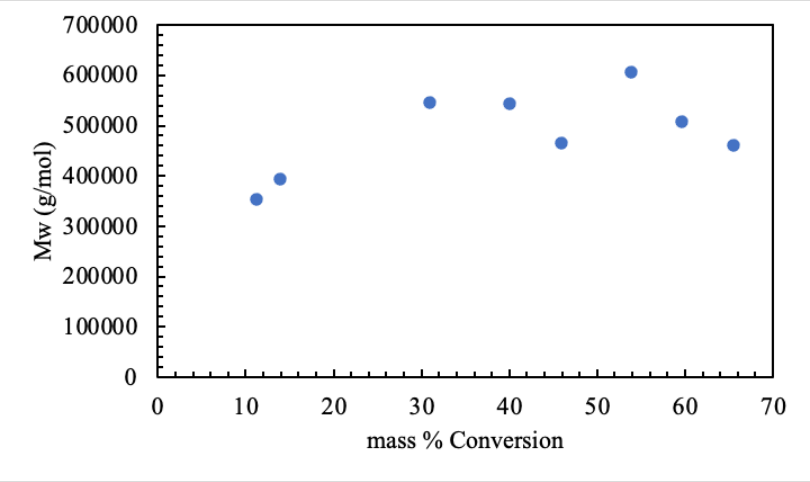

Figure 5.8: Weight-Average Molecular Weights versus Conversion for the Feed Composition of $f_{IA,0}$ = 0.1

Figure 5.8 shows the relationship between $\overline{M_w}$ and mass conversion for $f_{IA,0}$ =0.1. Between mass conversion of 0 and 30 percent, the $\overline{M_w}$ appears to increase fairly quickly, and then plateaus after 30% mass conversion at ~545 000 g/mol. The wide 'band' of data that occurs following stabilization (in terms of the molecular weight values) suggests that there is a lot of variability within this polymer system, especially between synthesis replicates. However, the trend generally follows what would be expected for free radical polymerization (which is a type of chain growth polymerization), as seen in Figure 5.9, where the sample quickly reaches its maximum molecular weight and then plateaus as conversion continues to increase. However, in the experimental results of Figure 5.8 (for $f_{IA,0}$ =0.1), the conversion where the plateau is reached is slightly higher than expected. That is, the fact that the molecular weight does not plateau until 30% seems somewhat unusual, since the polymer product should reach its maximum molecular weight almost instantaneously.

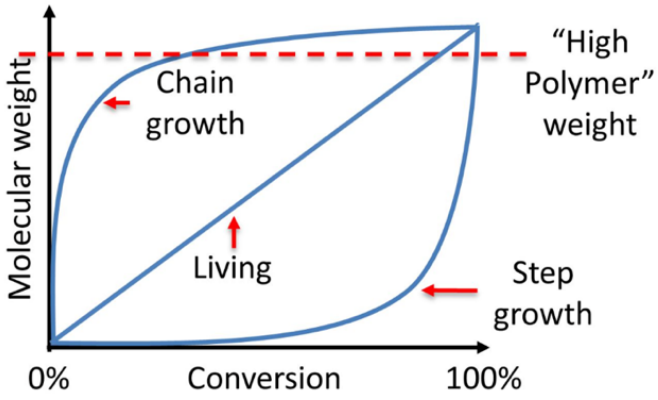

Figure 5.9: Typical Molecular Weight versus Conversion Profile for Chain Growth Polymerizations [51]

Figure 5.10 shows the relationship between $\overline{M_w}$ and mass conversion for $f_{IA,0}$ =0.2. These results do not follow the general trend shown in Figure 5.9; instead the data gradually increase linearly to a molecular weight of 207 000 g/mol at a conversion of 24.5%, and then quickly increases to a

molecular weight of 656 000 g/mol at 61.2%. This unexpected trend is investigated further in Chapter 6.

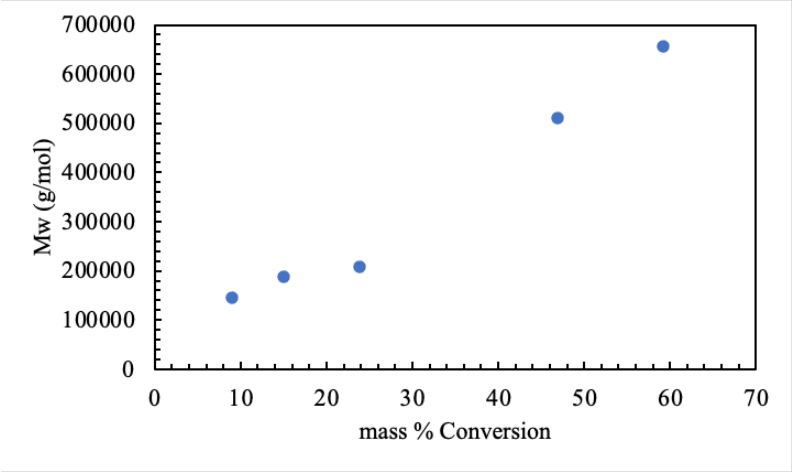

Figure 5.10: Weight-Average Molecular Weights versus Conversion for $f_{IA,0} = 0.2$

The specific refractive index increment (dn/dc) is an important parameter in molecular weight measurements using GPC. It is a parameter used by the refractive index detector to relate the refractive index measurement to the sample concentration, and is specific to the sample being run and the composition of the sample (for instance, the ratio of the comonomers in the copolymer will impact the dn/dc values). The dn/dc for itaconic acid and acrylamide systems has not been reported, however poly(acrylamide) has a dn/dc value of approximately 0.18 in water and poly(acrylic acid) has a dn/dc of approximately 0.15 in water [52]. Therefore, a dn/dc value in the range of approximately 0.15 to 0.18 is expected for the itaconic acid/acrylamide polymers. However, since the dn/dc value is not explicitly known, the molecular weight measurements are dependent on accurate polymer concentrations during GPC sample preparation. The dn/dc values, determined by the GPC software using the experimental (prepared) concentrations of the polymer samples, were typically found to be in the range of 0.18 to 0.24. These values seem reasonable

given the known dn/dc values for poly(acrylamide) and poly(acrylic acid), and the results further indicate that the GPC molecular weight measurements are accurate.

The final characterization method for the preliminary experiments was zeta potential. The samples were prepared as detailed in Section 4.3.3, with the zeta values listed here being an average of three measurements of the same sample. The samples prepared using the 10 mol% IA feed composition did not easily meet the quality criteria defined by the software and had to be completely re-run twice (in triplicate each time) until a value of -17.9 mV was measured, this error could have been because the sample concentration was lower than required. Also, as shown in Table 5.7, this sample had a larger standard deviation than the other formulations. The zeta potential of other two samples was -31.1 mV and -26.3 mV for samples prepared using $f_{IA,0}$ =0.2 and 0.3, respectively. These values are quite a bit lower than those measured for the commercial flocculants (recall Table 5.3; the samples synthesized from itaconic acid and acrylamide are all much closer to zero than -100 mV). These values could be smaller than the commercial samples due to the lower $\overline{M_w}$ and degree of polymerization. Since there is physically less of the charged monomer (itaconic acid) due to the lower molecular weights, it makes sense that there would be a lower net surface charge on the polymer.

Table 5.7: Zeta Potential for Itaconic Acid / Acrylamide Copolymers (n=3)

Feed Composition ($f_{IA,0}$)	**Conversion of Selected Sample (%)**	**Zeta Potential (mV)**	**Standard Deviation (mV)**
0.1	59.6	-17.9	+/- 5.3
0.2	59.3	-31.1	+/- 1.2
0.3	25.7	-26.3	+/- 4.2

Chapter 6. Optimization Experiments

The 20% itaconic acid (IA) feed composition was chosen as the most promising polymer sample synthesized to date, due to the fact that it had similar properties to the 10% IA feed composition samples but incorporated a higher amount of IA. It was hypothesized that this would allow for more of the anionic comonomers to be present, which would improve the electrostatic flocculation mechanism; this expectation is based on the composition determined through elemental analysis.

The highest $\overline{M_w}$ achieved for this formulation during the preliminary experiments was 656 000 g/mol, which was much lower than the commercial benchmarks determined in Section 5.4.1 (on the order of 10^7 g/mol). Additionally, a much lower zeta potential of -31 mV was observed for this formulation, in contrast to approximately -100 mV for the commercial benchmarks. These discrepancies motivated the following experiments, in an effort to move towards optimality by achieving polymer properties closer to the commercial benchmarks. This was done through an initiator concentration study detailed below in Sections 6.1 and 6.2.

6.1 Initiator Concentration Study

Since the total monomer concentration is limited by the solubility of itaconic acid in water (see discussion in Section 2.4) and was already near the maximum solubility limit, the initiator concentration was selected as the key variable to be optimized.

Using the data from the preliminary experiments, along with known experimental parameters such as monomer concentration and the molecular weight of the predicted repeating unit, a desired

molecular weight could be chosen, and the initiator concentration required to reach that molecular weight could theoretically be calculated using the relationship found in Section 2.5 (recall Equation 2.18). Two $\overline{M_n}$ were chosen as the targets: 10^6 g/mol and 10^7 g/mol. The former was chosen to provide a fairly close target to what was already being achieved, and the latter was chosen since it was close to the commercial benchmark. While the primary molecular weight characteristic investigated in Section 5.4 was the $\overline{M_w}$, it was anticipated that the PDI would be sufficiently narrow that an order of magnitude target would be sufficient. The calculated initiator concentrations were determined to be $5.5 \cdot 10^{-4}$ M for desired $\overline{M_n}$ of 10^6 g/mol, and $5.5 \cdot 10^{-6}$ M for desired $\overline{M_n}$ of 10^7 g/mol (see Appendix A for sample calculations).

6.2 Characterization of Synthesized Polymer

Both of the calculated initiator concentrations intended to achieve target molecular weight averages were polymerized with one replicate each. The rest of the experimental parameters, including total monomer concentration and polymerization temperature, were kept identical to the preliminary studies. The lowest initiator concentration ($5.5 \cdot 10^{-6}$ M) did not produce solid polymer within 24 hours for either replicate. This is likely due to the fact that as the initiator concentration is lowered, the rate of polymerization is also decreased to the point of where it becomes unfeasible for future scale-up and industrial use (recall Equation 2.5).

The moderate initiator concentration ($5.5 \cdot 10^{-4}$ M) allowed the formulation to polymerize, however it demonstrated that the rate of polymerization decreased with decreasing initiator concentration (as expected). Figure 6.1 shows a comparison of the conversion vs. time profiles using the original

initiator concentration (labelled I1) of 0.0022 M versus the new initiator concentration (labelled I2) of $5.5 \cdot 10^{-4}$ M. It is clear that the rate of polymerization is much slower when the lower initiator concentration is used, with the I1 reaching 10% mass conversion at about 90 minutes versus I2 reaching 10% conversion at about 250 minutes.

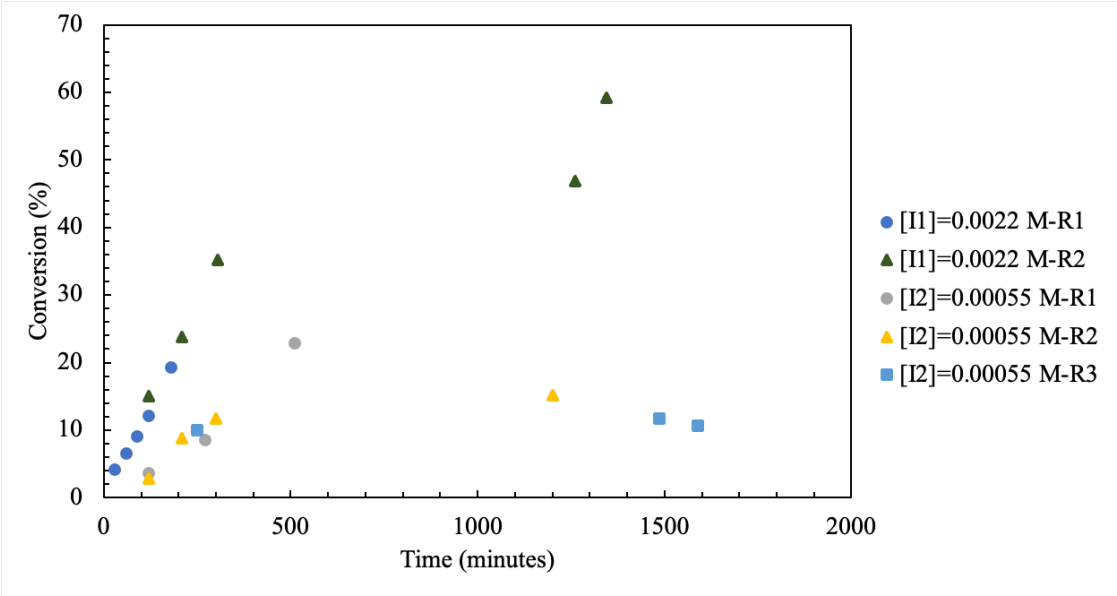

Figure 6.1: Comparison of Two Initiator Concentrations, I1 and I2, for the feed Composition of $f_{IA,0} = 0.2$

Figure 6.1 also shows that the conversion appears to reach a maximum of ~22% when the lower initiator concentration is used, as opposed to the original 60% conversion. There were also several data points (over all runs) that were identified as outliers at polymerization times above 1200 minutes. There has been a recurring issue with this copolymer system that at higher polymerization times (1200 minutes +), conversions begin to drastically decrease which is not physically possible. This was also observed with the experimental data for $f_{IA,0}$=0.3 (recall Figure 5.3), where outliers were also identified at higher polymerization times. This could be due to the isolation technique

not adequately precipitating the polymeric material out of the aqueous solution and should be investigated further in future work.

The $\overline{M_w}$ were also measured for the samples produced with the lower initiator concentration, using the methodology described in Section 4.3.2. A maximum $\overline{M_w}$ of 400 000 g/mol was measured at a 9.9% mass conversion, however the $\overline{M_w}$ varies between 200 000 g/mol and 400 000 g/mol over all conversion levels, up to the maximum conversion of 22.8%, as seen in Figure 6.2.

Even though the conversion data observed using this initiator concentration are less reliable due to the apparent decreasing conversion over time, the goal of increasing the $\overline{M_w}$ was somewhat successful as shown in Figure 6.2. Within the limited mass conversion obtained using the moderate initiator concentration ([I]= $5.5 \cdot 10^{-4}$ M), the majority of the samples had higher $\overline{M_w}$ than the higher initiator concentration ([I]=0.0022 M) at the same conversion level. However, due to the substantially decreased polymerization rate and the variability in the data (that is, the lack of meaningful trends within the data), this avenue of experimentation was not pursued further for this project.

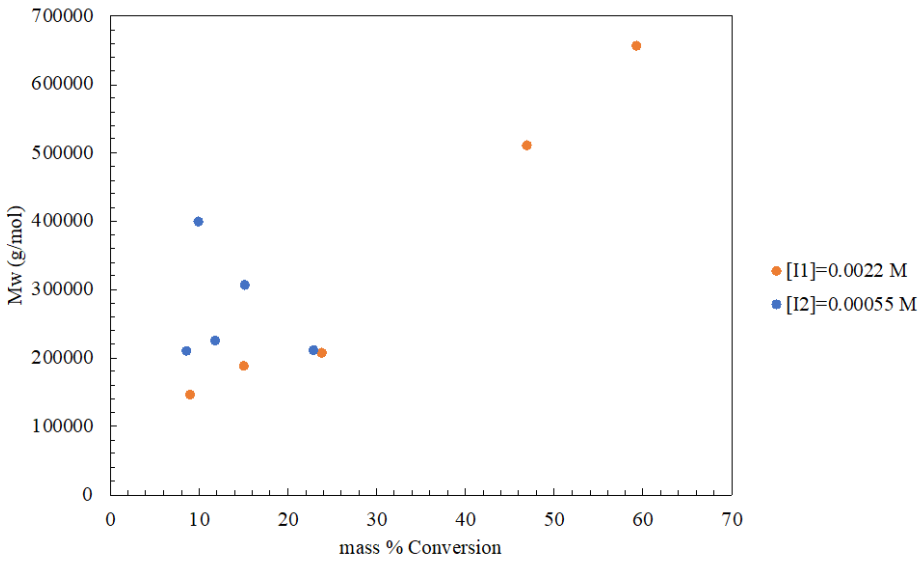

Figure 6.2: Comparison of Weight-Average Molecular Weights for Two Initiator Concentrations, I1 and I2, for the Feed Composition of $f_{IA,0}$= 0.2

Since lowering the initiator concentration did not present a feasible solution for increasing $\overline{M_w}$, the original initiator concentration ([I] = 0.0022 M) was re-evaluated to determine whether there was another way to increase the $\overline{M_w}$. Based on the preliminary results (recall Figure 5.10), it was observed that the $\overline{M_w}$ appeared to be increasing linearly with time for 20 mol % IA. This suggested that it would be theoretically possible to increase the polymerization time to achieve higher molecular weight averages or to verify that the $\overline{M_w}$ had stabilized. Therefore, the next step was to increase the polymerization time in an effort to increase the $\overline{M_w}$.

As shown in Figure 6.3, the conversion versus time relationship does not follow the expected trend, especially over long polymerization times. The conversion increases linearly until 42%, and then the increase slows as the conversion reaches 66%, after which there is an apparent decrease. Two data points from "R4" were identified as outliers due to experimental error, as conversions were extremely low; this may occur if the septa are not closed fully during degassing. The overall results

appear to be repeatable, as the same general trend is observed with different replicates. It is important to note that it is physically impossible for the conversion to decrease over time, however this could be due to variability between the samples; one might suggest that a "thick" (variable) plateau is reached between 50 and 60% conversion.

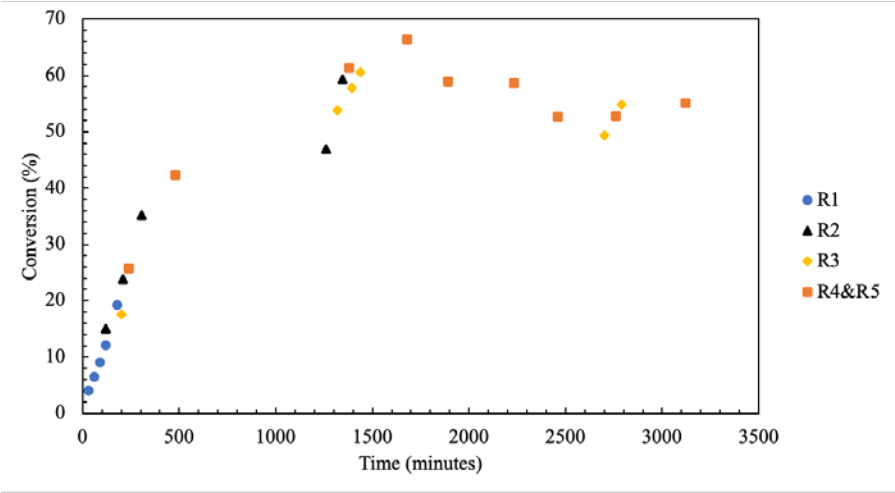

Figure 6.3: Extended Conversion versus Time Relationship for [I]=0.0022 M and $f_{IA,0}$ = 0.2

Using this extended copolymerization time, a maximum $\overline{M_w}$ of 706 981 g/mol at a conversion of 54.8% was observed, and the $\overline{M_w}$ stabilized between 600 000 and 700 000 g/mol (see Figure 6.4). It should also be noted that this relationship does not follow the expected trend of molecular weight versus time for chain growth polymerizations, as discussed in Chapter 5 (recall Figure 5.9). This could be due to the fact that $r_{IA} > 1$, therefore itaconic acid is more likely to react with itself first. As the itaconic acid monomer is consumed, which is a slow process as evidenced by the literature [27]), this can be explained by the linear trend observed in the lower conversion data in Figure 6.4 (between 0 and 23.8% conversion). Once the acrylamide monomer incorporation increases, there is a sudden increase between 23.8% and 46.9%, where the $\overline{M_w}$ rises from 207 000 g/mol to 511 000 g/mol. This is likely due to the fact that acrylamide reacts much more quickly than itaconic

acid. This can also be linked to the elemental analysis results, where the higher conversions demonstrated more acrylamide incorporation into the copolymer samples (see Table 5.5 and Figure 5.6). Ultimately, the $\overline{M_w}$ appear to stabilize between 650 000 and 700 000 g/mol.

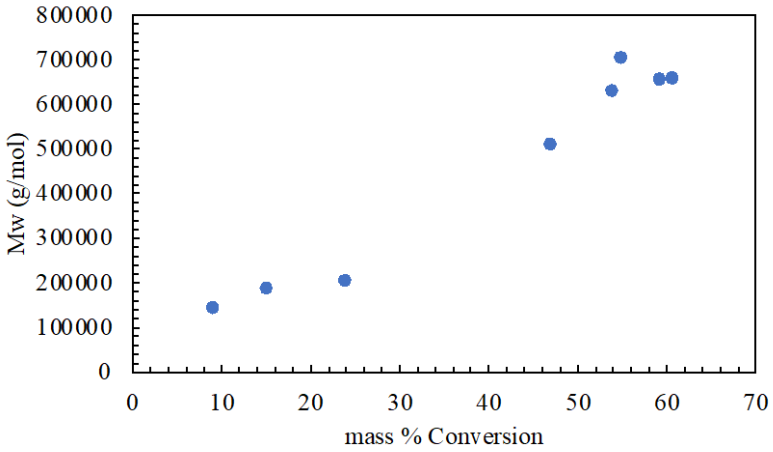

Figure 6.4: Extended Weight-Average Molecular Weights versus Conversion for [I]=0.0022 M and $f_{IA,0}$ = 0.2

6.3 Application Testing

One sample synthesized from each of the $f_{IA,0}$=0.1 and $f_{IA,0}$=0.2 feed compositions were taken to Halifax Water's Dartmouth Wastewater Treatment Facility for application testing, with help provided by a CWRS coop student Kayleigh Dunphy. The selected samples had $\overline{M_w}$ of 544 000 g/mol and 707 000 g/mol, respectively. The three commercially available polymer flocculants (characterized in Section 5.4.1) were also tested for comparison. All five samples were prepared at a concentration of 1 mg/ml in HPLC grade water and dissolved using magnetic stir bars at 500 rpm.

Eleven jars were prepared for analysis, each with 1 litre of influent (untreated) wastewater. Each of the five samples were tested with 2 replicates, and the eleventh jar was for the control that only contained aluminum sulphate coagulant (without any polymer flocculant). The jar testing parameters included a 30 second premixing stage at 240 rpm, followed by a 5 minute rapid mixing at 180 rpm where 125 μL of aluminum sulfate (coagulant) was added at the beginning. The 10-minute flocculation stage (slow mixing) at 40 rpm was next, where the polymer was added at the beginning of this stage at a dose of 2 mg/L. Finally, the settling stage was observed, with no mixing for 20 minutes. These parameters were recommended by wastewater treatment experts at Halifax Water as the standard testing parameters.

The untreated influent collected on the same day as the jar tests was characterized using a variety of measurements, all of which have been summarized in Table 6.1. These values can vary from day to day and provide a baseline for any future comparisons with other flocculation experiments.

Table 6.1: Influent Wastewater Characterization

Temperature	18.5 °C
pH	7.16
Turbidity	67.7 NTU
BOD	183.05 mg/L
COD	215 mg/L
Alkalinity	122 mg/L
Zeta Potential	-15.67 mV

The first property that was evaluated was the visual floc characterization. This essentially involved observing the size of the flocs that formed during the flocculation stage, as shown in Figure 6.5. It is clear that the commercial samples all formed large, well-defined flocs. In comparison, the itaconic acid/acrylamide copolymers showed no clear formation of flocs and performed similarly to the control (containing only aluminum sulphate). These tests were replicated with the same observations.

Figure 6.5: Visual Floc Characterization from Jar Tests (From Left to Right: Sample C, Sample A, $f_{IA,0} = 0.1$, Sample B, $f_{IA,0} = 0.2$, and the Control)

The next property to be evaluated was the zeta potential of the "treated" wastewater, with the results shown in Figure 6.6. All zeta potentials were negative; however the absolute values are shown here for ease of comparison. The ideal result is for the zeta potentials to approach 0, which represents that charge neutralization from the coagulant/flocculant has been effective. Each measurement for the commercial and synthesized samples (excluding influent and the control) reported in Figure 6.6 is an average of two replicated jar test results, each of which had 3 replicated zeta potential measurements. The influent and the control are based on an average of the three zeta measurements resulting from a single jar test. All of the samples decreased the zeta potential

compared to the influent, however there are no meaningful trends between the samples and the control.

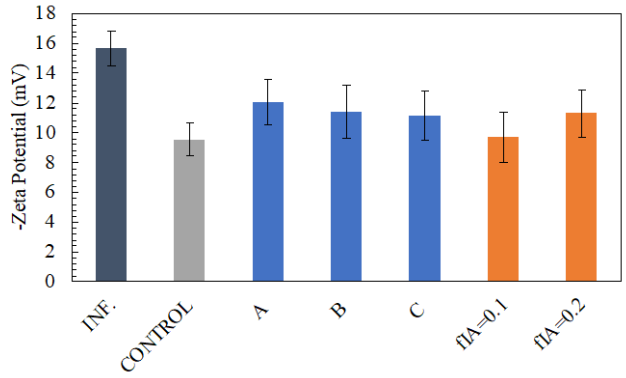

Figure 6.6: Zeta Potential Results from Jar Tests; Comparison of Influent, Commercial, and Novel IA/AAm Copolymers

The final characteristic that was evaluated was the turbidity, which describes the clarity of the wastewater sample. A turbidity of 0 NTU means that the water is clear, and a higher turbidity value indicates that solids are suspended in the water. The measurements shown in Figure 6.7 are an average of the turbidity measurements from the two replicate jar tests. It is evident that treatment with the commercial samples (A-C) greatly reduces the turbidity to around 2 NTU. It was also observed that the itaconic acid/acrylamide copolymers showed turbidity results that were nearly identical to the control (with just the aluminum sulphate) and were therefore not as effective as the commercial samples for wastewater treatment.

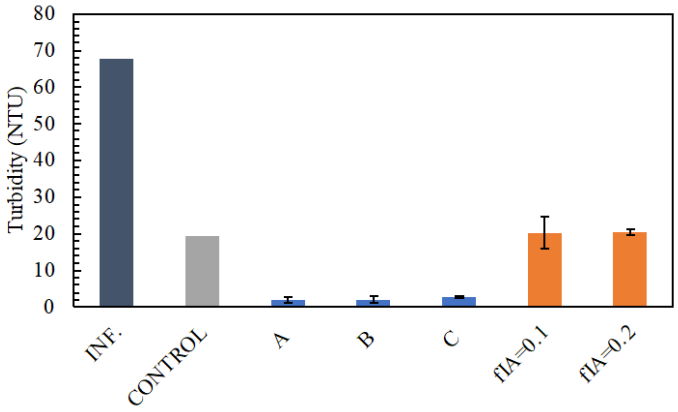

Figure 6.7: Turbidity Results from Jar Tests; Comparison of Influent, Commercial, and Novel IA/AAm Copolymers

These results confirm that the $\overline{M_w}$ of polymers for flocculation need to be well above 10^6 g/mol. The itaconic acid/acrylamide copolymers have not yet achieved sufficient flocculation, and further experimentation is required to increase the $\overline{M_w}$ closer to the commercial benchmark values.

Chapter 7. Conclusions and Recommendations for Future Work

7.1 Conclusions

Innovation within the water treatment industry will help to deal with the diverse nature of contaminants that are being found in wastewaters across different industries. Specifically, the production of novel custom polymer flocculants that can be tailored to specific contaminants could improve flocculation ability and allow for a smaller dosage of flocculants to be used. Also, as many monomers, such as acrylic acid, become unavailable due to the shift away from petroleum processes, alternative materials need to be researched. Itaconic acid has been identified as a potential alternative to acrylic acid in the production of anionic polymer flocculants, however much is still unknown about the itaconic acid and acrylamide copolymer system. This study looked at optimizing a polymerization procedure with the aim of better understanding the reaction kinetics of itaconic acid and acrylamide.

Successful synthesis of itaconic acid and acrylamide copolymers was achieved at $f_{IA,0}$= 0.1, 0.2 and 0.3, with the key polymer properties listed in Table 7.1. The values listed here are for the samples with the highest $\overline{M_w}$ from each feed composition. The zeta potentials for representative copolymer samples (not shown in Table 7.1) were found to be -17.9 mV, -31.1 mV, and -26.3 mV for $f_{IA,0}$= 0.1, 0.2 and 0.3, respectively.

Table 7.1: Characterization of IA/AAm Copolymers

$f_{IA,0}$	Conversion (%)	Cumulative Copolymer Composition ($\overline{F}_{IA}$)	Weight-Average Molecular Weight (g/mol)
0.1	53.8	0.21	605 490
0.2	54.8	0.35	706 981
0.3	14.3	0.47	193 216

The reactivity ratios were also estimated using newly collected data by applying the cumulative error-in-variables model, and it was determined that $r_{IA} = 1.4577$ and $r_{AAm} = 0.2914$. These results are in agreement with expected trends in the literature, however due to experimental limitations only lower feed compositions were used in the estimation. However, similar limitations have been reported in related copolymerization studies [24], suggesting that the limited data set may still be suitable for reactivity ratio estimation. Additionally, the model was validated using additional experimental data that had not been included in the estimation data.

This study demonstrated that the design framework proposed by Scott and Penlidis [1] can be used in the design of polymer flocculants for wastewater treatment. Through the application of the design framework, key variables such as the initiator concentration were identified and used to work towards optimal polymer properties. Additional work is needed to refine these polymeric materials for wastewater treatment; however this study provides a beneficial foundation and promising results for novel, custom-designed polymer flocculants.

7.2 Recommendations for Future Work

The short-term recommendations, which could be completed within four months and minimal experimental work, include:

- Study how the pH of the pre-polymer solution affects the reactivity ratios and incorporation of each of the comonomers. There is a narrow range, between pH 2 and 3.8, that is ideal for these comonomers and for this study they were observed to be between 2.09 and 2.4 for each of the feed compositions. Increasing the pH closer to 3 could impact the incorporation of acrylamide into the copolymer.

- Additional experiments should be performed with higher monomer concentrations at the lower feed compositions. The monomer concentration was kept constant between feed compositions in this study, which was limited by the highest IA feed composition and the solubility of IA in water. However, higher monomer concentration is expected to lead to an increase in molecular weight averages that can be achieved.

- The feed composition of $f_{IA,0}$=0.1 should be reinvestigated as it better aligns with the amount of charged comonomer incorporation found in the commercial samples.

- Further analysis and replication of molecular weight characterization using GPC would be useful for this copolymer system, especially to observe the trends at higher conversions. A study on the dn/dc values for these materials would also be beneficial for any future work, so that prepared concentration values could be validated.

- Identification of other polymer characteristics that would impact flocculation ability and zeta potential measurements, such as the charge density and microstructure of the polymer, would be beneficial to observe and understand the system more fully.

- For further iterations of the design framework, the key variables should be expanded to further understand the polymer system. These could include the reaction temperature and pH of the system.

The long-term recommendations, which could be completed within a year of additional experiments, include:

- Additional studies investigating why there is a higher incorporation of itaconic acid within this copolymer system, when acrylamide is known to be more reactive, would provide a better understanding of the complete system.

- Other methods of polymerization could be considered for this system, such as emulsion polymerization. This would help to mitigate the solubility issues encountered in this study and would also be useful in any future scale-up studies, as emulsion polymerization is widely used in industry to produce commercial polymeric materials.

- Investigate the potential to automate the design framework using machine learning or artificial intelligence to aid in Stage 1 for building prior or background knowledge of monomers for a specific application.

- The microstructure of itaconic acid and acrylamide copolymers should be characterized, in an effort to better understand how the polymerization parameters impact the resulting polymer microstructure.

- The isolation technique following polymer synthesis should be further investigated to determine the most appropriate non-solvent for this system. This would be useful for determining the reliability of the higher conversion data, especially at higher feed fractions of itaconic acid.

- Controlled radical polymerization could be utilized to further narrow the molecular weight distribution for samples synthesized using the $f_{IA,0}$=0.2 formulation. This technique helps to ensure that the polymer chains being synthesized are all similar in length, which would lower the PDI values for this system.

References

[1] A. Scott and A. Penlidis, "Design of Polymeric Materials: Experiences and Prescriptions," *The Canadian Journal of Chemical Engineering,* vol. 99, no. 1, pp. 5-30, 2020.

[2] A. Scott, M. Riahinezhad and A. Penlidis, "Optimal Design for Reactivity Ratio Estimation: A Comparison of Techniques for AMPS/Acrylamide and AMPS/Acrylic Acid Copolymerizations," *Processes,* vol. 3, pp. 749-768, 2015.

[3] C. Erbil, S. Özdemir and N. Uyanik, "Determination of the Monomer Reactivity Ratios for Copolymerization of Itaconic Acid and Acrylamide by Conductometric Titration Method," *Polymer,* vol. 41, no. 4, pp. 1391-1394, 1999.

[4] C. Erbil and N. Uyanik, "Monomer Reactivity Ratios of Itaconic Acid and Acrylamide Copolymers Determined by Using Potentiometric Titration Method," *European Polymer Journal,* vol. 36, pp. 2651-2654, 2000.

[5] "Polymer Water Treatment: How Coagulants and Flocculants Clean Wastewater," ClearWater Industries, 2021. [Online]. Available: https://clearwaterind.com/polymer-water-treatment-how-coagulants-and-flocculants-clean-wastewater/.

[6] V. Vajihinejad, S. P. Gumfekar, B. Bazoubandi, Z. Rostami Najafabadi and J. B. P. Soares, "Water Soluble Polymer Flocculants: Synthesis, Characterization, and Performance Assessment," *Macromolecular Materials and Engineering,* vol. 304, no. 2, 2018.

[7] B. Xiong, R. Dettam Loss, D. Shields, T. Pawlik, R. Hochreiter, A. L. Zydney and K. Manish, "Polyacrylamide Degradation and its Implications in Environmental Systems," *npj Clean Water,* vol. 1, no. 17, 2018.

[8] S. Waller, "Synthetic Polymeric Flocculants Aid Dewatering," Water Technology, 1 March 2000. [Online]. Available: https://www.watertechonline.com/wastewater/article/16191629/synthetic-polymeric-flocculants-aid-dewatering.

[9] O. V. Atamanova, E. I. Tikhomirova, A. S. Romanevich, A. S. Glubokaya and A. A. Podoksenov, "Improving the Quality of Wastewater Treatment by Flocculation," *Biology Bulletin,* vol. 49, pp. 1834-1839, 2022.

[10] S. Noppakundilograt, P. Nanakorn, W. Jinsart and S. Kiatkamjornwong, "Synthesis of Acrylamide/Acrylic Acid-based Aluminum Flocculant for Dye Reduction and Textile Wastewater Treatment," *Polymer Engineering and Science,* vol. 50, no. 8, pp. 1535-1546, 2010.

[11] "Acrylamide," American Chemical Society, 6 January 2020. [Online]. Available: https://www.acs.org/molecule-of-the-week/archive/a/acrylamide.html.

[12] "Acrylic Acid," Sigma-Aldritch, [Online]. Available: https://www.sigmaaldrich.com/CA/en/product/mm/800181.

[13] H. Kolya, D. Sasmal and T. Tripathy, "Novel Biodegradable Flocculating Agents Based on Grafted Starch Family For the Industrial Effluent Treatment," *Journal of Polymers and the Environment,* vol. 25, no. 2, pp. 408-418, 2017.

[14] H. Mittal, S. B. Mishra, A. Mishra, B. Kaith, R. Jindal and S. Kalia, "Preparation of Poly(acrylamide-co-acrylic acid)-Grafted Gum and its Flocculation and Biodegradation Studies," *Carbohydrate Polymers,* vol. 98, no. 1, pp. 397-404, 2013.

[15] B. Başaran, B. Çuvalcı and G. Kaban, "Dietary Acrylamide Exposure and Cancer Risk: A Systematic Approach to Human Epidemiological Studies," *Foods,* vol. 12, 2023.

[16] J.-H. Yang and C.-J. Lee, "Method of Removing Water from Products of Dehydration Reaction of 3-Hydroxypropioic Acid in Acrylic acid Process," *Computer Aided Chemical Engineering,* pp. 627-632, 2018.

[17] A. Rudin and P. Choi, The Elements of Polymer Science and Engineering, Elsevier/AP, 2013.

[18] C. S. Lee, J. Robinson and C. M. Fong, "A Review on Application of Flocculants in Wastewater Treatment," *Process Safety and Environmental Protection,* vol. 92, pp. 489-508, 2014.

[19] "Flocculation: Control Particle Size Distribution for Confident Process Development," Mettler-Toledo, [Online]. Available: https://www.mt.com/ca/en/home/applications/L1_AutoChem_Applications/L2_ParticleProcessing/flocculation.html.

[20] M. Daifa, E. Shmoeli and A. J. Domb, "Enhanced Flocculation Activity of Polyacrylamide-based Flocculant for Purification of Industrial Wastewater," *Polymers for advanced technologies,* vol. 30, no. 10, pp. 2636-2646, 2019.

[21] D. V. Dixon and J. Soares, "Molecular Weight Distribution Effects of Polyacrylamide Flocculants on Clay Aggregate Formation," *Colloids and Surfaces A: Physicochemical and Engineering Aspects,* vol. 649, 2022.

[22] A. Pandey, C. Larroche and C. Soccol, "Chapter 18: Solid-State Fermentation for the Production of Organic Acids," in *Current Developments in Biotechnology and Bioengineering: Current Advances in Solid State Fermentation*, Elsevier, 2018, pp. 415-434.

[23] B.-E. Teleky and D. C. Vodnar, "Biomass-Derived Production of Itaconic Acid as a Building Block in Specialty Polymers," *Polymers,* vol. 11, no. 6, 2019.

[24] S. Cummings, Y. Zhang, N. Kazemi, A. Penlidis and M. Dubé, "Determination of Reactivity Ratios for the Copolymerization of Poly(acrylic acid-co-itaconic acid)," *Journal of Applied Polymer Science,* vol. 133, no. 40, 2016.

[25] M. Moo-Young, M. Butler, K. Kirimura, Y. Honda and T. Hattori, "3.14: Gluconic and Itaconic Acids," in *Comprehensive Biotechnology (second edition)*, Elsevier Science, 2011, pp. 143-147.

[26] "Itaconic Acid," Millipore-Sigma, [Online]. Available: https://www.sigmaaldrich.com/CA/en/product/aldrich/i29204.

[27] L. Sollka and K. Lienkamp, "Progress in the Free and Controlled Radical Homo- and Co-Polymerization of Itaconic Acid Derivatives: Toward Functional Polymers with Controlled Molar Mass Distribution and Architecture," *Macromolecular Rapid COmmunications,* vol. 42, no. 4, 2020.

[28] W. Ma, L. Yang, Y. Wu, Y. Zhang, C. Liu, J. Maa and B. Suna, "Synthesis, Characterization and Properties of a Novel Environmentally Friendly Ternary Hydrophilic Copolymer," *RSC Advances,* vol. 13, no. 17, pp. 11685-11696, 2023.

[29] A. Chiloeches, R. Cuervo-Rodríguez, F. López-Fabal, M. Fernández-García, C. Echeverría and A. Muñoz-Bonilla, "Antibacterial and Compostable Polymers Derived from Biobased Itaconic Acid as Environmentally Friendly Additives for Biopolymers," *Polymer Testing,* vol. 109, 2022.

[30] J. Zhang, Z. Gong, C. Wu, T. Li, Y. Tang, J. Wu, C. Jiang, M. Miao and D. Zhang, "Itaconic Acid-Based Hyperbranched Polymer Toughened Epoxy Resins with Rapid Stress Relaxation, Superb Solvent Resistance and Closed-loop Recyclability," *Green Chemistry,* vol. 24, pp. 6900-6911, 2022.

[31] M. S. Birajdar, H. Joo, W.-G. Koh and H. Park, "Natural Bio-based Monomers for Biomedical Applications: A Reivew," *Biomaterials Research,* vol. 25, no. 8, 2021.

[32] A. Hevekerl, A. Kuenz and K.-D. Vorlop, "Filamentous Fungi in Microtiter Plates—an Easy Way to Optimize Itaconic Acid Production with Aspergillus terreus," *Applied Microbiology and Biotechnology,* vol. 98, pp. 6983-6989, 2014.

[33] T. Klement and J. Büchs, "Itaconic Acid – A Biotechnological Process in Change," *Bioresource Technology,* vol. 135, pp. 422-431, 2013.

[34] T. Mostafa, H. Naguib, M. Sabaa and S. Mokhtar, "Graft Copolymerization of Itaconic Acid onto Chitin and its Properties," *Polymer International,* vol. 54, no. 1, pp. 221-225, 2004.

[35] H. Jiang, M. Zhou, D. Pan and L. Tan, "The Influence of Ultrahigh Molecular Weight Polyacrylonitrile on the Copolymerization of Acrylonitrile with Itaconic Acid and on the Rheological Properties of the Resulting Polyacrylonitrile Solutions," *Textile Research Journal,* vol. 85, no. 20, pp. 2188-2195, 2015.

[36] R. Balilvand, A. Nodehi, J. K. Rad and M. Atai, "Solution Photo-Copolymerization of Acrylic Acid and Itaconic Acid: The Effect of Polymerization Parameters on Mechanical Properties of Glass Ionomer Cements," *Journal of the Mechanical Behaviour of Biomedical Materials,* vol. 126, 2022.

[37] S. Nagai, "Polymerization and Polymers of Itaconic Acid Derivatives. V. The Copolymerization Reactivity of Itaconic Acid in an Aqueous Solution," *Bulletin of the Chemical Society of Japan,* vol. 36, no. 11, pp. 1373-1544, 1963.

[38] C. Erbil, B. Terlan, Ö. Akdemir and A. T. Gökçeören, "Monomer Reactivity Ratios of N-Isopropylacrylamide–Itaconic Acid Copolymers at Low and High Conversions," *European Polymer Journal,* vol. 45, no. 6, pp. 1728-1737, 2009.

[39] M. Pulat and H. Eksi, "Determination of Swelling Behavior and Morphological Properties of Poly(acrylamide-co-itaconic acid) and Poly(acrylic acid-co-itaconic acid) Copolymeric Hydrogels," *Journal of Applied Polymer Science,* vol. 102, no. 6, pp. 5994-5999, 2006.

[40] D. Foungfung, S. Phattanarudee, N. Seetapan and S. Kiatkamjornwong, "Acrylamide–Itaconic Acid Superabsorbent Polymers and Superabsorbent Polymer/mica Nanocomposites," *Polymers for Advanced Technologies,* vol. 22, no. 5, pp. 635-647, 2011.

[41] N. Seetapan, N. Srisithipantakul and S. Kiatkamjornwong, "Synthesis of Acrylamide-co-(Itaconic Acid) Superabsorbent Polymers and Associated Silica Superabsorbent Polymer Composites," *Polymer Engineering and Science,* vol. 51, no. 4, pp. 764-775, 2011.

[42] A. Scott and A. Penlidis, "Computational Package for Copolymerization Reactivity Ratio Estimation: Improved Access to the Error-in-Variables Model," *Processes,* vol. 6, no. 1, 2018.

[43] C. Hagiopol, "Estimation of Reactivity Ratios," in *Copolymerization: Toward a Systematic Approach*, Kluwer Academic, 1999, pp. 19-95.

[44] N. Kazemi, T. Duever and A. Penlidis, "A Powerful Estimation Scheme with the Error-in-Variables Model for Nonlinear Cases: Reactivity Ratio Estimation Examples," *Computational Chemical Engineering,* vol. 48, pp. 200-208, 2013.

[45] N. Kazemi, T. A. Duever and A. Penlidis, "Reactivity Ratio Estimation from Cumulative Copolymer Composition Data," *Macromolecular Reaction Engineering,* vol. 5, no. 9-10, pp. 385-403, 2011.

[46] A. Paril, A. Alb, A. Giz and H. Catalgil-Giz, "Effect of Medium pH on the Reactivity Ratios in Acrylamide Acrylic Acid Copolymerization," *Journal of Applied Polymer Science,* vol. 103, pp. 968-974, 2006.

[47] R. Simič, J. Mandal, K. Zhang and N. Spencer, "Oxygen Inhibition of Free-Radical Polymerization is the Dominant Mechanism behind the "mold effect" on Hydrogels," *Soft Matter,* vol. 17, no. 26, pp. 6394-6403, 2021.

[48] M. Riahinezhad, N. Kazemi, N. McManus and A. Panlidis, "Optimal Estimation of Reactivity Ratios for Acrylamide/Acrylic Acid Copolymerization," *Journal of Polymer Science,* vol. 51, pp. 4819-4827, 2013.

[49] N. Kazemi, T. A. Duever and A. Penlidis, "Design of Experiments for Reactivity Ratio Estimation in Multicomponent Polymerizations Using the Error-In-Variables Approach," *Macromolecular Theory and SImulations,* vol. 22, no. 5, pp. 261-272, 2013.

[50] S. Bednarz, A. Wesołowska-Piętak, R. Konefał and T. Świergosz, "Interactions between Persulfate Initiated Free-radical Polymerization of itaconic acid: Kinetics, End-gro(acrylamide)–poly(itaconic acid) and Cerium(IV)–nitrilotriacetic Acid Redox Pair in the Synthesis of Acrylamide and Itaconic Acid Homo- and Copolymers," *European Polymer Journal,* vol. 106, pp. 63-71, 2018.

[51] E. S. Sterner, Polymer Science Learning Center, 2003. [Online]. Available: https://pslc.ws/macrog/synth.htm.

[52] J. Brandrup, E. H. Immergut and E. A. Grulke, "Specific Refractive Index Increments of Polymers in Dilute Solutions," in *Polymer Handbook*, pp. 557-559.

[53] "Chemical Book," [Online]. Available: https://www.chemicalbook.com/SpectrumEN_97-65-4_1hnmr.htm.

Appendix A – Sample Calculations and Supplemental Data

A.1 Elemental Analysis Supplemental Data

Table A.1 and A.2 show the data collected from the elemental analyzer (weight percents of carbon, hydrogen, nitrogen, and sulfur). The weight percent of oxygen is also reported, however this value was not collected from the elemental analyzer but was instead calculated as the remaining balance. A sample calculation of oxygen weight percent is presented below:

$$\text{weight \% O} = 100 - \text{mass \% C} - \text{mass \% H} - \text{mass \% N} - \text{mass \% S} \quad \text{(A.1)}$$
$$\text{weight \% O} = 100 - 39.94 - 6.524 - 12.18 - 0.231 = 41.125\ \%$$

Table A.1: Mass Percent Measurements of Carbon, Hydrogen, Nitrogen, and Sulfur from Elemental Analysis for Commercial Samples

Sample	wt % C	wt % H	wt % N	wt % S	wt % O
A	39.94	6.524	12.18	0.231	41.125
B	38.9	6.222	12.93	0.116	40.832
C	37.18	6.093	11.71	0.215	44.802

Table A.2: Mass Percent Measurements of Carbon, Hydrogen, Nitrogen, and Sulfur from Elemental Analysis For IA/Aam Copolymers

Sample	wt % C	wt % H	wt % N	wt % S	wt % O
C1-5 R1	43.84	6.715	12.25	0.138	37.057
C1-2 R2	45.05	6.612	12.35	0.178	35.81
C1-4 R2	46.66	6.859	12.62	0.148	33.713
C1-2 R3	47.47	6.648	12.41	0.217	33.255
C1-3 R3	47.68	6.777	12.13	0.222	33.191
C1-3 R3*	47.76	6.796	12.26	0.198	32.986
C1-6 R3	46.96	6.815	12.15	0.178	33.897
C1-7 R3	46.36	6.809	12.99	0.216	33.625
C2-2 R1	46.08	6.348	8.73	0.208	38.634
C2-2 R1*	46.1	6.323	8.79	0.137	38.65
C2-3 R1	45.63	6.272	8.57	0.154	39.374
C2-4 R1	45.52	6.205	9.31	0.197	38.768
C2-5 R1	46.13	6.33	9.25	0.233	38.057
C2-1 R2	46.75	6.447	8.47	0.294	38.039
C2-2 R2	45.82	6.383	8.94	0.235	38.622
C2-3 R2	45.92	6.336	9.05	0.196	38.498
C2-4 R2	46.66	6.836	10.9	0.214	35.363
C2-5 R2	45.59	6.717	11.54	0.222	35.831
C3-1 R3	43.11	6.112	6.74	0.394	43.644
C3-2 R3	43.22	6.276	6.71	0.249	43.545

C3-3 R3	43.46	6.237	7.01	0.191	43.102

*These values are sample characterization replicates completed to validate results.

The sample names are in the form of C(feed composition)-Sample R(replicate#). So, the second sample from an experiment with $f_{IA,0}$=0.1 in the first replicate experiment would be C1-2 R1.

A.2 Cumulative Composition Calculations

Cumulative copolymer composition was calculated using the data presented in Table A.1 and A.2, with the content of carbon, hydrogen, nitrogen, and oxygen being used in the approximate empirical formulas. The sulfur measured below 0.5 % of the mass across all samples and was therefore considered negligible in the determination of the approximate empirical formulas. Hydrogen was not included in the calculation of the composition since the data could be easily influenced by the amount of moisture in the atmosphere. A sample calculation is presented below in Table A.3.

Table A.3: Cumulative Copolymer Composition Calculation using C1-5

Element	Weight %	# of moles	Mole ratio
C	43.84	3.650	4.173
H	6.715	6.663	7.619
N	12.25	0.875	1.000
S	0.138	0.004	0.005
O	37.057	2.316	2.648

The weight percent is collected directly from the elemental analysis software. The number of moles is calculated by dividing the weight % by the elemental molecular weights, shown in Equation A.1. Nitrogen was selected as the basis for the mole ratio calculations as it is only present in acrylamide. The mole ratios are determined by dividing the number of moles for each of the elements by the number of moles of nitrogen (see Equation A.2).

$$\#\text{ of moles C} = 43.84\text{ wt\% C}\left(\frac{1\text{ mol C}}{12.011\text{ g C}}\right) = 3.650\text{ mol C} \tag{A.1}$$

$$\text{C mole ratio} = \frac{\#\text{ of moles C}}{\#\text{ of moles N}} = \frac{3.650}{0.875} = 4.173 \tag{A.2}$$

The mole ratios were used to determine the approximate empirical formulas by rounding to the nearest whole number.

The relative amount of carbon was then used to calculate how many moles of each comonomer are present in the synthesized copolymer. Assuming there are A moles of acrylamide and B moles of itaconic acid:

$$\text{C} = 3\text{A} + 5\text{B} \tag{A.3}$$

$$\text{N} = \text{A}$$

$$B = \frac{\text{C mole ratio} - 3A}{5} = \frac{4.173 - 3(1)}{5} = 0.235 \quad \text{(A.4)}$$

$\overline{F_{IA}} = \frac{B}{A+B} = \frac{0.235}{1+0.235} = 0.190$ for this copolymer sample.

A.3 Initiator Concentration Calculations

Equation 2.20 in Section 2.5.3 was used to calculate a lumped constant (including $k_p, f, k_d,$ and k_t) from the preliminary experiments. The equation has been rearranged to lump the constants together, shown in Equation A.5.

$$\frac{k_p}{2(fk_dk_t)^{\frac{1}{2}}} = \frac{\nu[I]^{\frac{1}{2}}}{[M]} \quad \text{(A.5)}$$

Using the highest molecular weight achieved for $f_{IA,0}$=0.2 (at the time of this calculation), and the known molecular weight of the repeat unit, which is a weighted average of the comonomers based on the average composition of the copolymer ($0.35*M_{IA} + 0.65*M_{AAm}$), the number-average degree of polymerization was calculated.

$$\overline{DP_n} = \frac{511\,493}{(0.35 \cdot 130.099) + (0.65 \cdot 71.08)} = 5575.67 \quad \text{(A.6)}$$

The kinetic chain length was then calculated for termination by combination, which is the most common form of termination for free radical polymerization. This was achieved by dividing the number average degree of polymerization in half.

$$\nu = \frac{\overline{DP_n}}{2} = \frac{5575.67}{2} = 2787.83 \quad \text{(A.7)}$$

The calculated kinetic chain length, known initiator concentration, and known monomer concentration used in the preliminary experiments was then used to calculate a predicted constant for this system.

$$\frac{k_p}{2(fk_dk_t)^{\frac{1}{2}}} = \frac{2787.83[0.0022]^{\frac{1}{2}}}{[0.9]} = 145.29 \quad \text{(A.8)}$$

This lumped constant was then used to calculate initiator concentrations for desired molecular weights of 10^6 g/mol and 10^7 g/mol. A new kinetic chain length was calculated for the desired molecular weights, combining *steps A.6 and A.7 above.*

$$\nu_1 = \frac{\left(\frac{10^6}{(0.35 \cdot 130.099)+(0.65 \cdot 71.08)}\right)}{2} = 5450.38 \quad \textit{(A.8)}$$

$$\nu_2 = \frac{\left(\frac{10^7}{(0.35 \cdot 130.099)+(0.65 \cdot 71.08)}\right)}{2} = 54503.84 \quad \text{(A.8)}$$

The initiator concentrations were then calculated for each of the desired molecular weights, using a rearranged Equation 2.20.

$$[\mathrm{I}]_1 = \left(\frac{145.29[\mathrm{M}]}{\nu}\right)^2 = \left(\frac{145.29[0.9]}{5450.38}\right)^2 = 5.5 \cdot 10^{-4}\ \mathrm{M} \quad \text{(A.9)}$$

$$[\mathrm{I}]_2 = \left(\frac{145.29[\mathrm{M}]}{\nu}\right)^2 = \left(\frac{145.29[0.9]}{54503.84}\right)^2 = 5.5 \cdot 10^{-6}\ \mathrm{M} \quad \text{(A.10)}$$

These concentrations were then converted to the mass of initiator (KPS) for a 100 mL polymer solution.

$$\mathrm{m}_{\mathrm{I},1} = [\mathrm{I}]_1 \left(\frac{270.322\ \mathrm{g\ KPS}}{1\ \mathrm{mol\ KPS}}\right)\left(\frac{1000\ \mathrm{mg}}{1\ \mathrm{g}}\right)\ (0.1\ \mathrm{L}) = 14.87\ \mathrm{mg} \quad \text{(A.11)}$$

$$\mathrm{m}_{\mathrm{I},2} = [\mathrm{I}]_2 \left(\frac{270.322\ \mathrm{g\ KPS}}{1\ \mathrm{mol\ KPS}}\right)\left(\frac{1000\ \mathrm{mg}}{1\ \mathrm{g}}\right)\ (0.1\ \mathrm{L}) = 0.15\ \mathrm{mg} \quad \text{(A.12)}$$

Appendix B – Nuclear Magnetic Resonance Results

Nuclear magnetic resonance (^{1}H-NMR) was completed on the $f_{IA,0}$=0.2 stock solution (that is, the comonomer solution prior to polymerization) as well as a polymerized sample from $f_{IA,0}$=0.2 to verify that itaconic acid was being incorporated into the copolymer. A Bruker AV300 NMR spectrometer was used to collect the spectra. The stock solution was scanned as it was prepared (see Section 4.2), and only contained the comonomers, itaconic acid and acrylamide, in HPLC H_2O. For the polymerized sample, 10 mL of the $f_{IA,0}$=0.2 stock solution was transferred to a sealed reaction vial with initiator (KPS) added at a concentration of 0.0022 M. The sample was degassed for 45 minutes, and then placed in a water bath at 50°C for 10 hours.

Due to the similarities in the structures of the two monomers, many of their peaks overlap. However, there are three peaks that can be attributed solely to itaconic acid, as they did not appear in the spectra for pure acrylamide. These have been denoted with black arrows in Figure B.1 (a), which shows the full spectrum, as well as in Figure B.1 (b), which shows a zoomed in spectrum between 3.5 and 4.5 ppm to see the peaks more clearly. The two peaks identified in Figure B.1(b) are associated with the carbon double bond that is present in the monomer (recall Figure 2.8 in Section 2.4) [53].

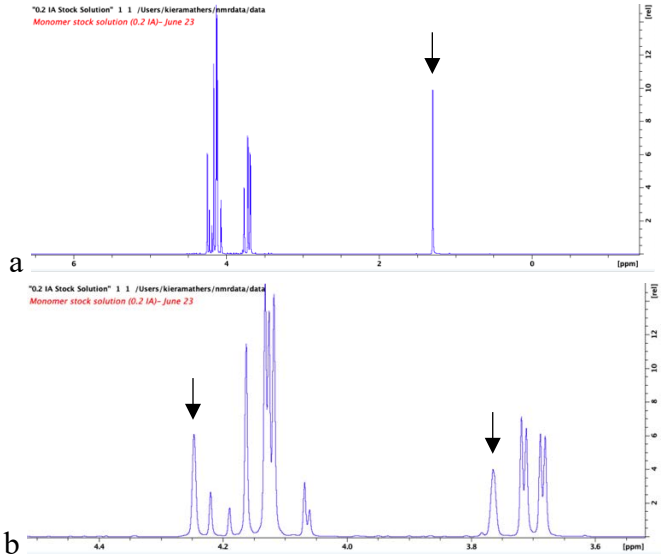

Figure B.1: (a) Full ^{1}H-NMR Spectrum for the Monomer Stock Solution of $f_{IA,0}$ = 0.2; (b) Enlarged Spectrum between 3.5 and 4.5 ppm to Identify Itaconic Acid Peaks

Figure B.2 shows the NMR spectrum for a sample of $f_{IA,0}$=0.2 solution that had been polymerized for 10 hours at 50°C in an NMR tube. This was done to investigate how the monomer peaks changed as the monomers were incorporated into the copolymer. It can be seen in Figure B.2 that all three itaconic acid peaks that were identified in Figure B.1 decreased following polymerization.

The two peaks identified in Figure B.1 (b) that were associated with the carbon double bond have completely disappeared. Because of the overlap of itaconic acid peaks and acrylamide peaks, it is difficult to use these spectra to verify the incorporation of acrylamide. It does appear that some of the other peaks from the stock solution change or decrease slightly, which could be due to the double bond of acrylamide decreasing. However, these results, along with the elemental analysis results (see Section 5.4.2), show that both itaconic acid and acrylamide are being incorporated into the synthesized copolymers. The wider peaks seen in Figure B.2 (a) are likely correlated to the copolymer being formed.

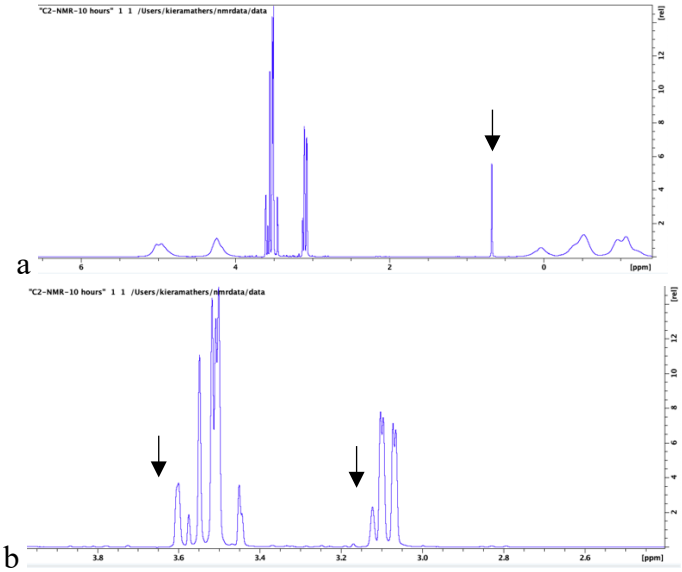

Figure B.2: (a) Full ^{1}H-NMR Spectrum for $f_{IA,0}$ = 0.2 Polymerized in an NMR Tube for 10 hours at 50 °C; (b) Enlarged Spectrum to Identify Itaconic Acid Peaks